GENERAL ⊕ ELECTRIC

GENERAL ELECTRIC COMPANY
CORPORATE RESEARCH AND DEVELOPMENT

Schenectady, N.Y.

AD734936

YTTRALOX CERAMIC LASER

ANNUAL REPORT

June 1, 1970 - May 31, 1971

Contract No.: N00014-70-C-0360

Program Code No.: OD10

Principal Investigators:

C. D. Greskovich
K. N. Woods

Sponsored by

Advanced Research Projects Agency
ARPA Order No. 1587

Submitted by

General Electric Company
Corporate Research and Development
Schenectady, New York 12301

DDC
RECEIVED
JAN 4 1972
B

DISTRIBUTION STATEMENT A

Approved for public release;
Distribution Unlimited

S-71-1085

52

<u>YTTRALOX</u> <u>CERAMIC</u> <u>LASER</u>

ANNUAL REPORT

June 1, 1970 - May 31, 1971

Contract No.: N00014-70-C-0360

Program Code No.: OD10

Principal Investigators:
    C. D. Greskovich
    K. N. Woods

FOREWORD

This work was carried out in the Metallurgy and Ceramics Laboratory
and the General Physics Laboratory of the General Electric Company Corporate
Research and Development under U. S. Navy Contract N00014-70-C-0360 entitled
"Yttralox Ceramic Laser."

The work was administered under the direction of Dr. Arthur Diness
from June 1, 1970 to May 31, 1971.

The authors acknowledge the contributions of the following individuals
to the program: Dr. J. C. Almasi and J. P. Chernoch for laser data and
interpretation, C. O'Clair for ceramic processing procedures and heat treatments
and M.F. Ciccarelli for assistance with the scanning electron microscope.

ABSTRACT

The oxalate and sulfate processes can produce Nd-doped Yttralox of high
optical quality. Although the sulfate process was not successful in producing
a Yttralox laser because of impurities in the Y_2O_3 powder, the oxalate process
yielded higher purity powder and in conjunction with a ball-milling procedure
enabled the reproducible fabrication of Yttralox rods which exhibited lasing
action.

The two major optical defects which have been identified in sintered
Yttralox are pores and a finely dispersed second phase. The second phase
appears to be removed by prolonged firing at temperatures between 2000 and 2200°C.
By ball-milling the calcined oxalate powder, Yttralox ceramic can be made with
a residual porosity between 10^{-6} and 10^{-7}. The majority of the pores are between
1/2 and 5µ and the overall pore size distribution can be directly related to
changes in ceramic processing.

Although sulfur is picked up as an impurity during the ball-milling
operation and forms a grain boundary decoration phase which contributes to
light scattering losses during lasing, the presence of this grain boundary
phase can permit pore elimination to a level which is generally two orders of
magnitude lower than in uncontaminated Yttralox.

Four neodymium-doped Yttralox rods prepared from ball-milled oxalate
powder exhibited lasing action. The lasing threshold values ranged between
60 and 28 joules and could be correlated to a first approximation with the
presence of porosity and a finely dispersed second phase. The loss coefficient
for the rod with the smallest threshold value was of the order of 2% per cm
and an efficiency of about 0.1%.

TABLE OF CONTENTS

TITLE PAGE

FOREWORD

ABSTRACT

LIST OF ILLUSTRATIONS

LIST OF ILLUSTRATIONS (Continued)

LIST OF TABLES

I.   INTRODUCTION

Yttralox® ceramic was invented at the General Electric Corporate Research and Development in 1964. This polycrystalline, oxide ceramic material--made by relatively conventional ceramic processing techniques--has a cubic crystal structure which is comprised of 90% Y_2O_3 and 10% ThO_2 or ZrO_2 in solid solution. The ThO_2 (or ZrO_2) functions as a grain growth inhibitor during sintering, permitting the attainment of a nearly pore-free ceramic body.[1,2] This material is transparent between 0.25 and 9.5μ with no absorption bands. Ideally, Yttralox ceramic is a clear, isotropic medium that is free from light scattering inclusions. In practice, the current state-of-the-art processing yields materials with occasional pores or other inhomogeneities.

Processing ceramic bodies that are completely free from pores and secondary phases is a longstanding technological objective to which much effort has been devoted over the last two decades. Although many of the useful properties of various ceramic materials could be enhanced by achieving a state of theoretical density and phase purity, only a few ceramics have been produced that closely approach this state. Lucalox® and Yttralox ceramics, and the IRTRAN series of hot pressed materials are in this category. The key to eliminating pores during sintering (without pressure) while maintaining phase purity is to inhibit or reduce exaggerated grain growth.[2] By inhibiting grain growth, vacancy diffusion can occur along grain boundaries and thus the porosity can be eliminated. The function of MgO in Lucalox alumina and of ThO_2 (or ZrO_2) in Yttralox ceramics is to cause such reduction of grain boundary mobility. In each case the sintering agents form a solid solution with the base oxide during the process, and lose their identity as a phase, although probably are adsorbed at the grain boundaries.

Neodymium-doped Yttralox ceramic is attractive as a laser material because it is expected to yield a higher energy output than either Nd-doped YAG or glass. The use of Nd^{+3} as a fluorescent center in laser hosts has a principal advantage of providing a low threshold of stimulated emission at 1.078μ and places a premium on optical homogeneity and low cavity loss. Numerous glass compositions and the crystal YAG are currently the most important host materials utilizing Nd^{+3} fluorescence for laser action. Glass can be made in larger sizes with excellent optical homogeneity, and being amorphous, has the inherent properties of high energy storage capability (low gain) and low thermal conductivity. On the other hand, YAG crystals are expensive and limited in size by crystal growth considerations. They have a relatively high thermal conductivity and a low energy storage capability (high gain). For these reasons, glass is favored for high energy Q-switched pulses while YAG is best suited to C.W. applications. Using the conventional rod design, high average pulsed power cannot be produced with either host. Yttralox ceramic, whose properties are intermediate between those of glass and YAG, has the potential for achieving a higher average pulsed power than either glass or YAG.

II. GOALS OF THE YTTRALASE PROGRAM

The long range goal of the current program is to develop the necessary technology for reproducibly fabricating a laser host material with both high peak and high average power characteristics. During the first year's contract, the overall goal was to evaluate Yttralox ceramic for these characteristics. (90% Y₂O₃), 10% ThO₂)or ZrO₂) in solid solution.)

Before such an evaluation could be made, it was estimated that the optical perfection of Yttralox must be improved by at least an order of magnitude. The major efforts of the first year's contract were to (1) seek to understand the sintering process with respect to the kinetics of porosity change, (2) develop a process to reproducibly fabricate Yttralox of improved optical quality, (3) evaluate Yttralase as a potential laser material by means of optical measurements, and (4) fabricate five laser rods of the best quality possible for delivery to the sponsor.

During the last quarter of the contract, the overall goal of evaluating Yttralox for lasing action was performed on five Nd-doped Yttralox rods. The results indicate that Yttralox ceramic is indeed a promising host material for high peak and high average power lasing action.

III. PROGRESS IN SINTERING THEORY

Studies on the early stages of sintering in MgO-doped Al O were done in conjunction with this program. Linde-A alumina was chosen as a model material because of its uniform particle size (0.3μ) and because there is a substantial amount of information on the sintering of Al_2O_3.[3,4,5] Since the experimental and theoretical results described are applicable to any ceramic system, these results are pertinent to the Yttralox program.

Powder compacts of alumina doped with 0.25 wt % MgO were prepared with variable relative green densities between 0.31 and 0.50. Shrinkage kinetics at 1270°C and 1370°C (see Figs. (1) and (2), respectively) were obtained by taking a series of photographs of the compacts.

The experimental results show that a series of different shrinkage curves can be generated for given powder simply by changing the green density of the compact. The higher the green density the higher is the shrinkage rate. In addition the values of the shrinkage slopes on a log shrinkage versus log time plot range from about 0.29 to 0.38 at 1270°C and from 0.27 to 0.47 at 1370°C. The variation in shrinkage rate and slope as a function of the green density of the compacts cannot be understood by the conventional model for the initial stages of sintering.
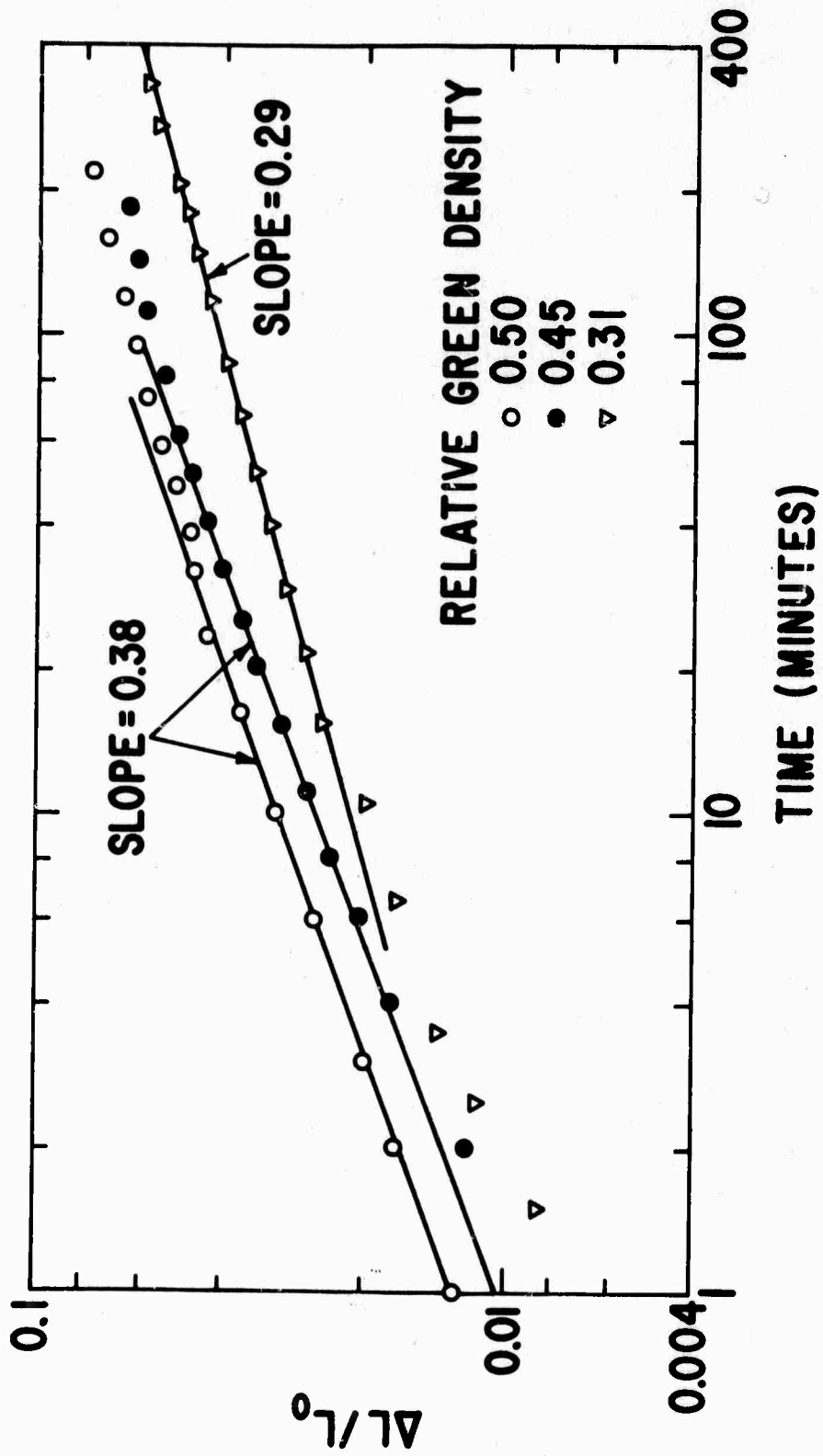
Figure 1. Effect of Green Density on Shrinkage Kinetics of Alumina Doped with 0.2 wt.% MgO at 1270°C

-4-
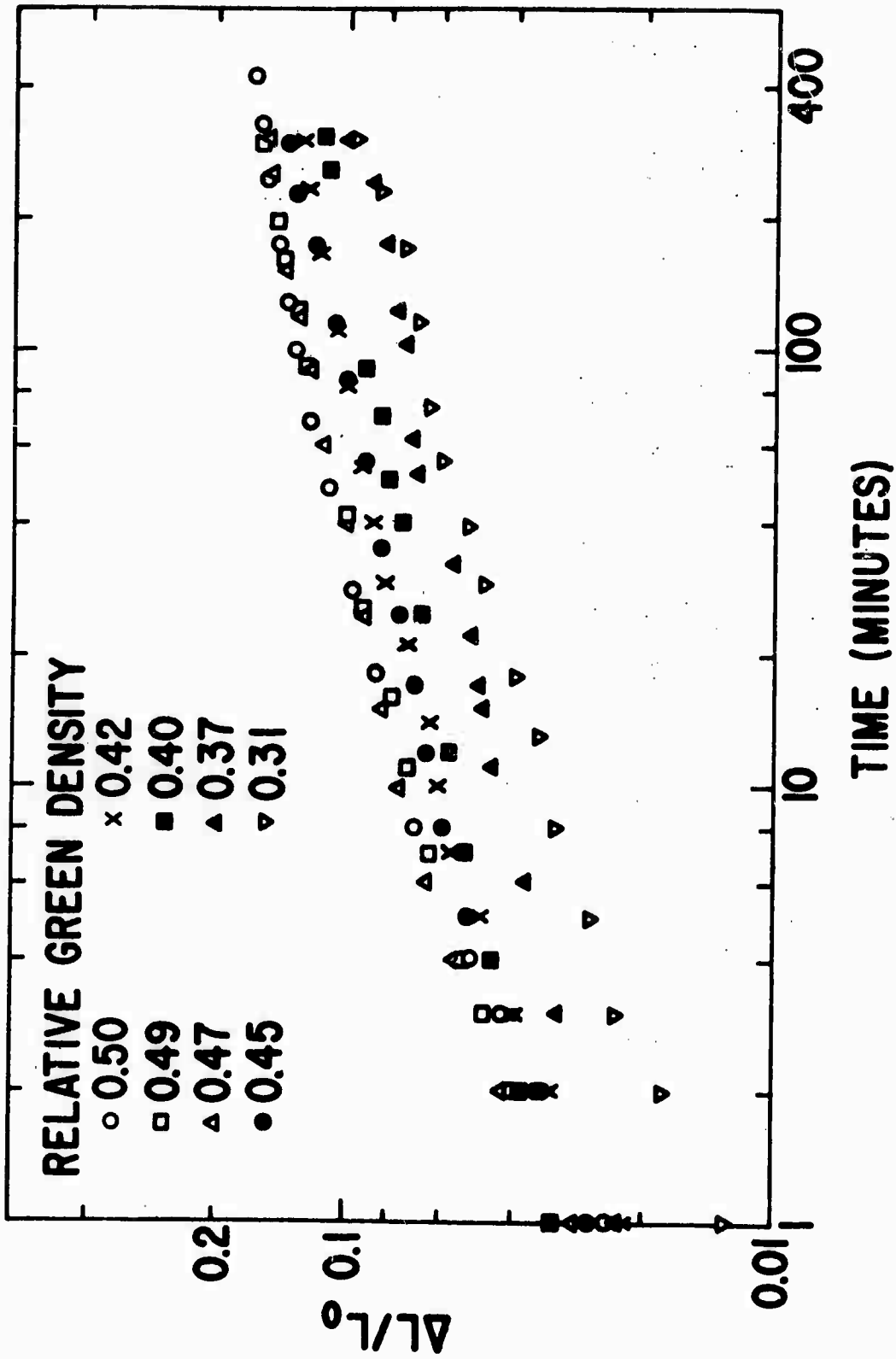
Figure 2. Effect of Green Density on Shrinkage Kinetics of
Alumina Doped with 0.2 wt. % MgO at 1370°C

The experimental data can be understood if there is a predominance of surface diffusion contributing to the neck growth between contacting particles before shrinkage begins. Wilson and Shewmon[6] and Prochazka and Coble[7] have pointed out the importance of surface diffusion in the sintering of Al_2O_3. Substitution of an average dimension of the pores bounded by contacting particles at the shrinkage temperature is a good representation of the ill-defined radius of curvature of the neck surface.

The excess concentration of vacancies (ΔC) in the immediate vicinity of a pore surface can be expressed by rewriting the Kelvin equation in its generalized form,

$$\Delta C = \frac{V_m C_o \gamma}{RT} \left(\frac{dA}{dV}\right) \tag{1}$$

where V_m is the molar volume, C_o is the vacancy concentration at the center of the grain boundary which is assumed to be a planar surface, γ is the surface free energy and dA/dV is the change in surface area of the pore with respect to its volume change. Since the driving force for shrinkage is approximately $\Delta C/X$ (where X is the radius of the circular neck between contacting particles), the greater the curvature the greater will be the flux of vacancies to the grain boundary (vacancy sink). A distribution of pore sizes in a powder compact has some average curvature which is prevailing at the time shrinkage begins. The mathematical determination of the average curvature is a complex geometrical problem which has been discussed by Hillert,[8] in his treatment of grain growth. To a first approximation we shall make the simplest presupposition that

$$\left(\frac{dA}{dV}\right)_{ave} \approx \frac{\beta}{\ell_p} \tag{2}$$

where β is a geometrical shape factor and ℓ_p is the average dimension of the pores or the average pore size. This average pore size will be a function of the packing density in the green compact and decreases with an increase in green density because the number of small pores increases with an increase in particle coordination number. Since the shrinkage rate can be shown to be inversely proportional to the now proposed average pore dimension, the shrinkage rate should increase with an increase in bulk density of the compacts, explaining part of the experimental results.

A modified form of Johnson and Clark's[9] shrinkage model can be developed with the assumptions that (1) there is no grain growth, (2) $X \gg l_p/2$, (3) the radius of curvature in their model is approximated by $l_p/2$, and (4) $3/l_p$ changes very slowly for shrinkages up to $\approx$ 6%. The introduction of these assumptions into the mathematical treatment leads to the following shrinkage equation for a mechanism of grain boundary diffusion:

$$\frac{\Delta L}{L_o} \approx \left(\frac{2b\gamma D_b \Omega \beta}{r^3 kT l_p}\right)^{1/2} t^{1/2} \tag{3}$$

where $\Delta L/L_o$ = fractional shrinkage, b = width of the enhanced diffusion zone at the grain boundary, D_b = self diffusion coefficient along the grain boundary, Ω = vacancy volume, r = initial particle size, kT = thermal energy and t = time. Equation (3) reveals that the shrinkage rate (quantity in brackets) is inversely proportional to the average pore size and the cube of the particle size. The increase in shrinkage rate with an increase in relative green density found in this study is thought to arise from the decreasing average pore size between contacting particles. Finally, although the shrinkage kinetics should approximate a $t^{1/2}$ law, pore growth and grain growth will change the time exponent in Eq. (3).

In summary, the consideration of the mechanism of pore removal leads to the conclusion that an ideal green ceramic compact should contain a uniform distribution of the smallest, uniformly-sized particles and voids. The introduction of one large pore (as a void at a packing fault caused by powder agglomerates) will decrease the diffusion flux of vacancies because the excess vacancy concentration is proportional to the reciprocal of the pore radius. Finally, since the diffusion coefficient depends exponentially on temperature, the higher the temperature the faster is the rate of densification of a sintering body.

IV. PROGRESS OF YTTRALASE PROGRAM

The reader whose main interest is in the current processing technique may want to proceed directly to the section entitled "Oxalate Process". Efforts to improve the sulfate technique, which is discussed in the next section, were terminated during the Fourth Quarter of this contract. Although the sulfate technique produced the first laser rod two years ago, drastic improvements in the material produced by the oxalate process make the latter process far more promising.

A. Sulfate Process

The sulfate process for making Yttralase can be briefly summarized as follows. Yttrium oxide powder is stirred into a filtered aqueous solution of thorium and neodymium sulfates. After thorough mixing, heat is applied to

drive off the water. The resulting powder, in which individual yttrium oxide particles are coated with very fine thorium and neodymium sulfate particles, is then calcined in air at 1000°C to convert the sulfates into oxides. This mixed oxide power is pressed into shape, calcined once more in air at 1350°C to drive off residual sulfur, and fired in hydrogen at temperatures above 2100°C to obtain transparency.

1. Powder Purity

A persistent problem inherent to the sulfate process is the starting purity of the commercially purchased yttrium oxide powder. The purity of this powder (99.99%) is specified in terms of its total rare earth components. Non-rare earth impurities are generally not reported in the analysis.

Careful examination of different lots of Y_2O_3 powder from several different domestic suppliers revealed that all contained a small number of non-white particles in the white Y_2O_3 powder. The color of these particles ranged from yellowish-orange to black. The black particles in one particular lot (Kerr McKee) were isolated and identified as hematite (Fe_2O_3). Spectro-chemical analysis of impurity particles in several of the other lots revealed high levels of Al and Si, possible contaminants from furnace brick.

One difficulty in obtaining a true chemical analysis of the Y_2O_3 powder is that the impurity particles are relatively few in number. A sample to be submitted for analysis must therefore be very large to ensure a true representation of the overall lot composition. The largest impurity particles were screened from the Y_2O_3 powder, and the results of spectrochemical analysis on these impurity particles is tabulated in Table I.

It is strongly suspected that much of the residual porosity, in samples made by the sulfate process is due to discrete impurity particles. A reduction in residual porosity occurred when the starting Y_2O_3 powder was screened through -140 mesh nylon screen to remove the largest impurity particles. Since the screening technique only removes particles larger than 100 microns, techniques for dissolving, filtering, and reprecipitating the Y_2O_3 powder would have to be developed to remove impurity particles smaller than that size. Alternatively, one might start with a water soluble yttrium compound, such as Yttrium sulfate, which could be dissolved, filtered, dried and calcined to yield a possibly higher purity Y_2O_3 powder.

2. Y_2O_3 Powder Characteristics

Y_2O_3 powders from five different commercial suppliers were examined during the course of the contract. A 5 gm sample of each powder was die-pressed to 38,000 psi. After measuring the green density of each pressed pill,

TABLE I

PERCENT IMPURITIES IN PARTICLES SCREENED FROM 50 gm. Y_2O_3 POWDERS

(Screen Mesh = -140)

	Molycorp	Research Chemicals	Kerr McKee	Alfa	Michigan Chemicals
Al	0.1	High	Low Medium	0.1	0.05
Ba	<0.05	ND*	<0.05	<0.05	<0.05
Ca	<0.05	ND*	<0.05	<0.05	<0.05
Cr	<0.001	ND*	0.005	<0.001	<0.001
Co	<0.001	ND*	<0.001	<0.001	<0.001
Cu	<0.001	ND*	0.002	<0.001	0.01
Fe	0.003	Medium	0.05	0.003	0.03
Pb	0.002	ND*	<0.001	<0.001	<0.001
Mg	0.01	ND*	<0.001	0.02	0.01
Mn	<0.001	ND*	0.002	<0.001	0.001
Ni	<0.001	ND*	0.007	<0.001	<0.001
K	<0.01	ND*	**	0.02	<0.01
Si	0.2	High	Low Medium	Medium	0.1
Na	<0.01	ND*	**	0.01	<0.01
Sr	<0.02	ND*	<0.02	<0.02	<0.02
Sn	<0.001	0.1	<0.001	<0.001	<0.001
Ti	0.01	Low Medium	0.005	0.005	0.003
V	<0.001	ND*	<0.001	<0.001	<0.001
Zn	<0.1	ND*	<0.1	<0.1	<0.1
Zr	<0.005	0.5	<0.005	0.02	0.005

* Not detected, very limited sample
**Insufficient sample to run alkalies

the samples were fired for 15 hours at 2100°C in dry H_2. The shrinkage that occurred for each sample during this sintering treatment is plotted vs. green density in Fig. 3. This graph shows the wide range of green densities and shrinkage characteristic of commercially available Y_2O_3 powders. The sintering treatment allowed each sample to reach greater than 99% theoretical density.

Two Y_2O_3 powders, Molycorp and Research Chemicals, were selected for more careful study. Samples of the powder were ultrasonically dispersed in an aqueous electrolyte, and cumulative particle size distributions were measured with a Coulter Counter. The lower limit of the measurement was 0.8μ. The derivative of the cumulative distribution curve for each sample is reproduced in Fig. 4. These derivative curves, which are representative of the actual particle size distribution, show that the Research Chemicals powder has a larger average particle size and a larger range of particle sizes than the Molycorp powder.

Scanning electron micrographs of ultrasonically dispersed Molycorp and Research Chemicals powders are shown in Fig. 5. The angular and laminated shape of the particles is similar for each powder, but the average particle size is distinctively larger in the Research Chemicals powder.

The effect of the die-pressing pressure on the green density and sintering characteristics of these two powders is shown in Fig. 6. The green density was measured for each of four different pressing pressures. All the samples were then fired for 15 hours at 1500°C and the shrinkage measured. The same samples were then given an additional sintering treatment of 21 hours at 1800°C and the shrinkage measured. The sample density ρ after each sintering treatment was calculated from the measured shrinkages by the formula

$$\rho = \rho_g \frac{1}{\left(1 - \frac{\Delta L}{L_o}\right)^3} \tag{4}$$

where

ρ_g = the as-pressed green density
L_o = original sample length in one dimension
ΔL = change in sample length during sintering.

As shown in Fig. 6, the green density of the Research Chemicals powder is higher than that of the Molycorp powder at each pressing pressure. The broader particle size distribution of the Research Chemicals powder apparently permits closer packing of the fine particles into the interstices between the larger particles.
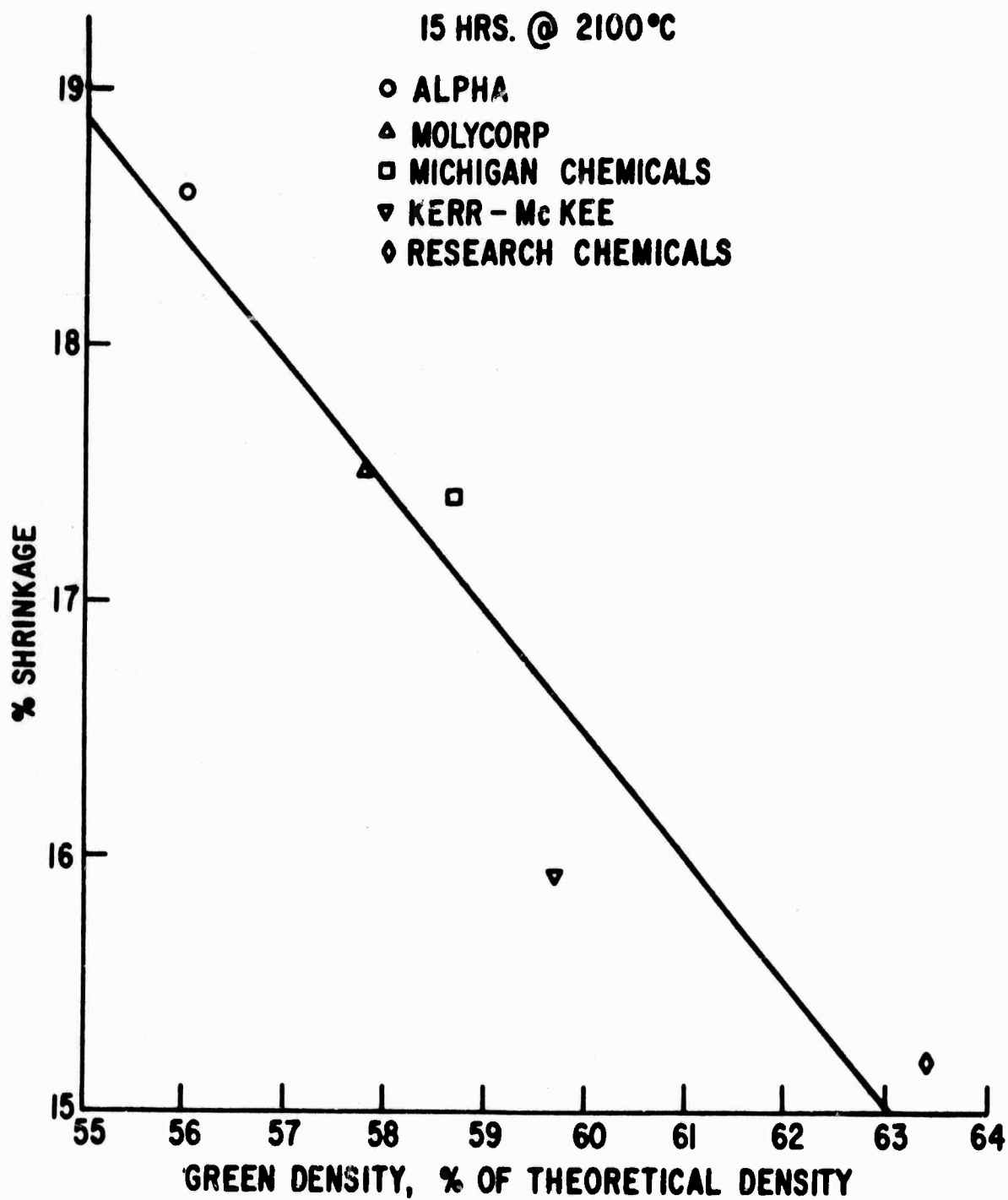
Figure 3. Shrinkage versus Green Density for five Y_2O_3 Powders Pressed to 38,000 psi and Sintered for 15 Hours at 2100°C in H_2
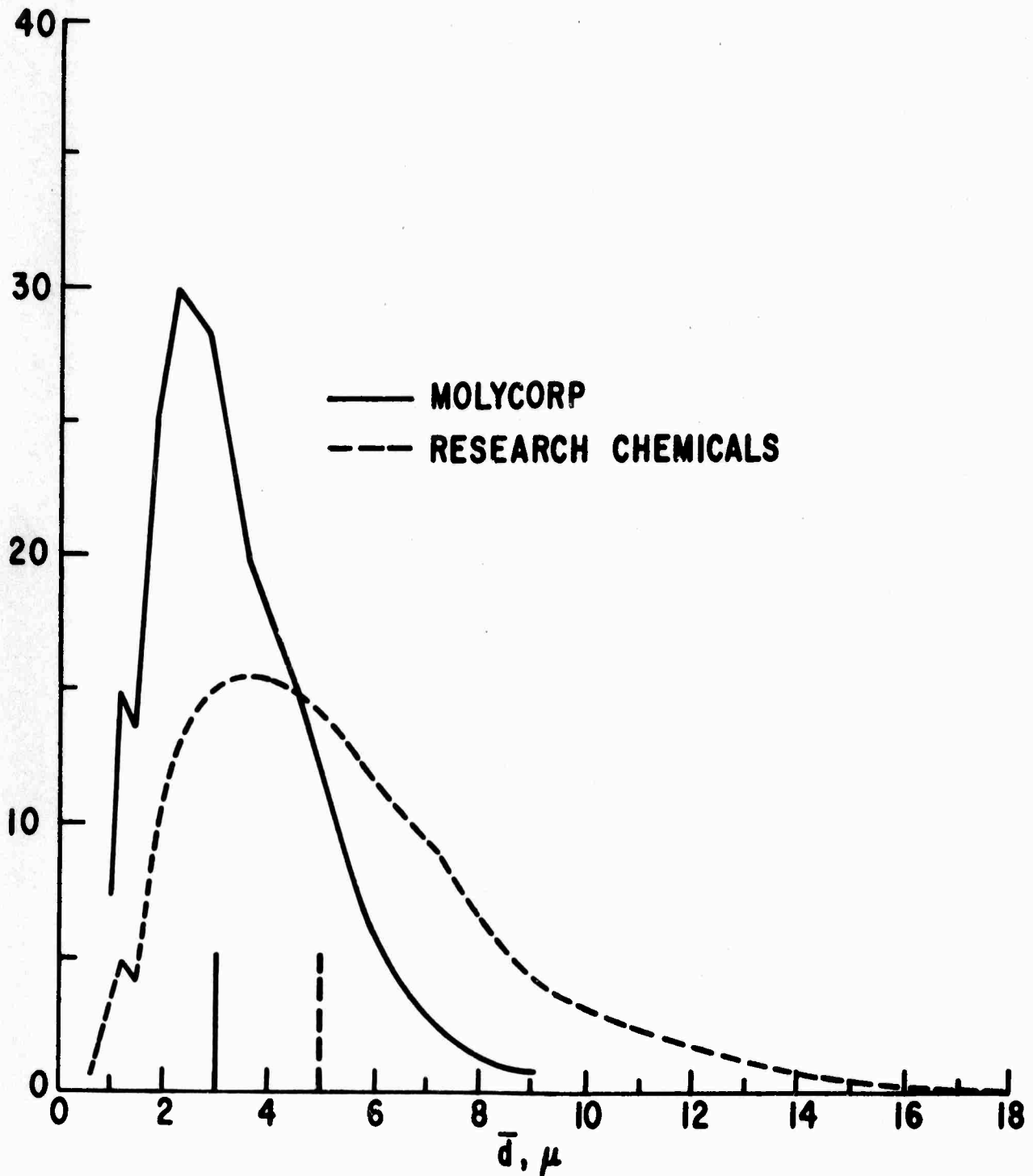
Figure 4. Particle Size Distribution Plotted as Frequency (in arbitrary units) versus Particle Diameter for Two Commercial Y_2O_3 Powders. Average Particle Size is Shown by Vertical Lines at 3 and 4 Microns
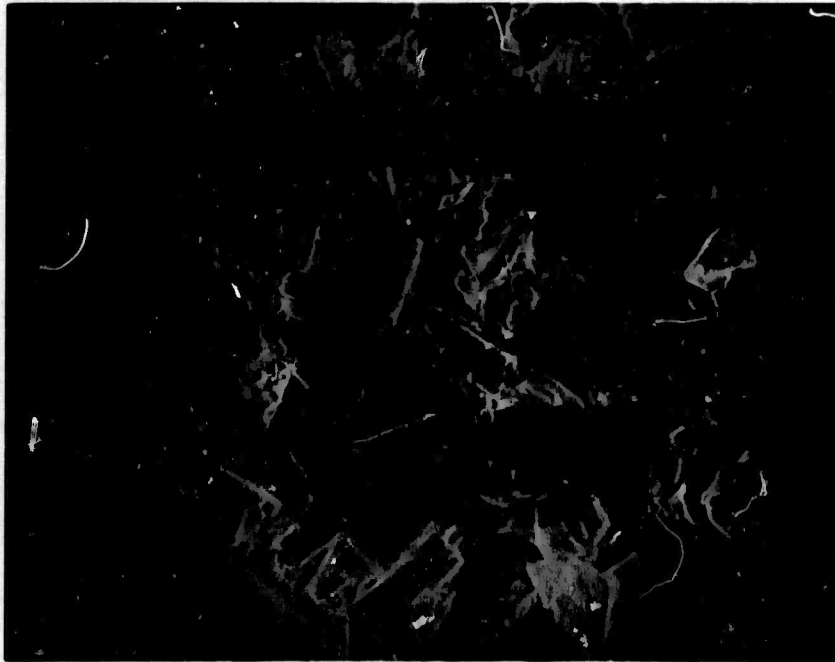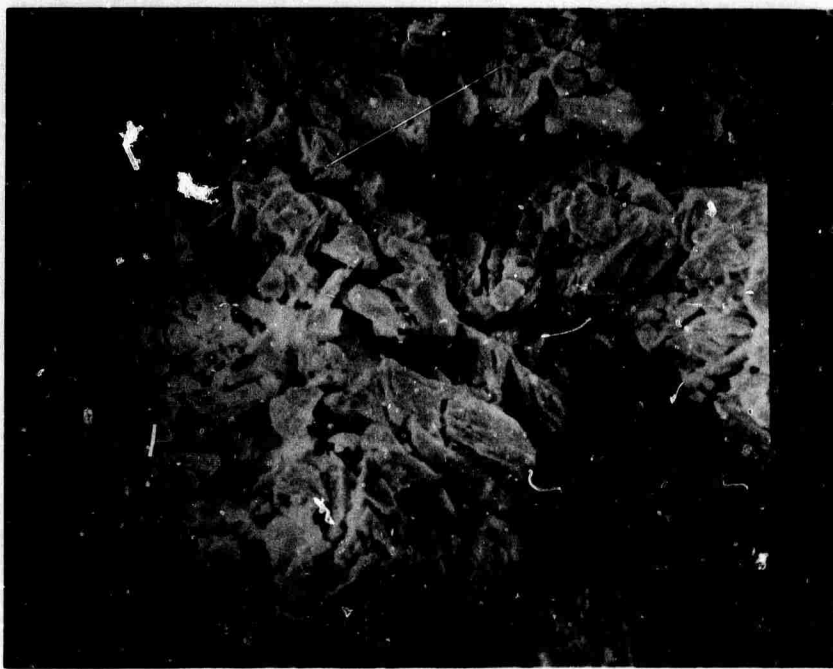
Figure 5. Scanning Electron Micrographs of Two Commercial Y_2O_3
Powders a) Molycorp, b) Research Chemicals X2000
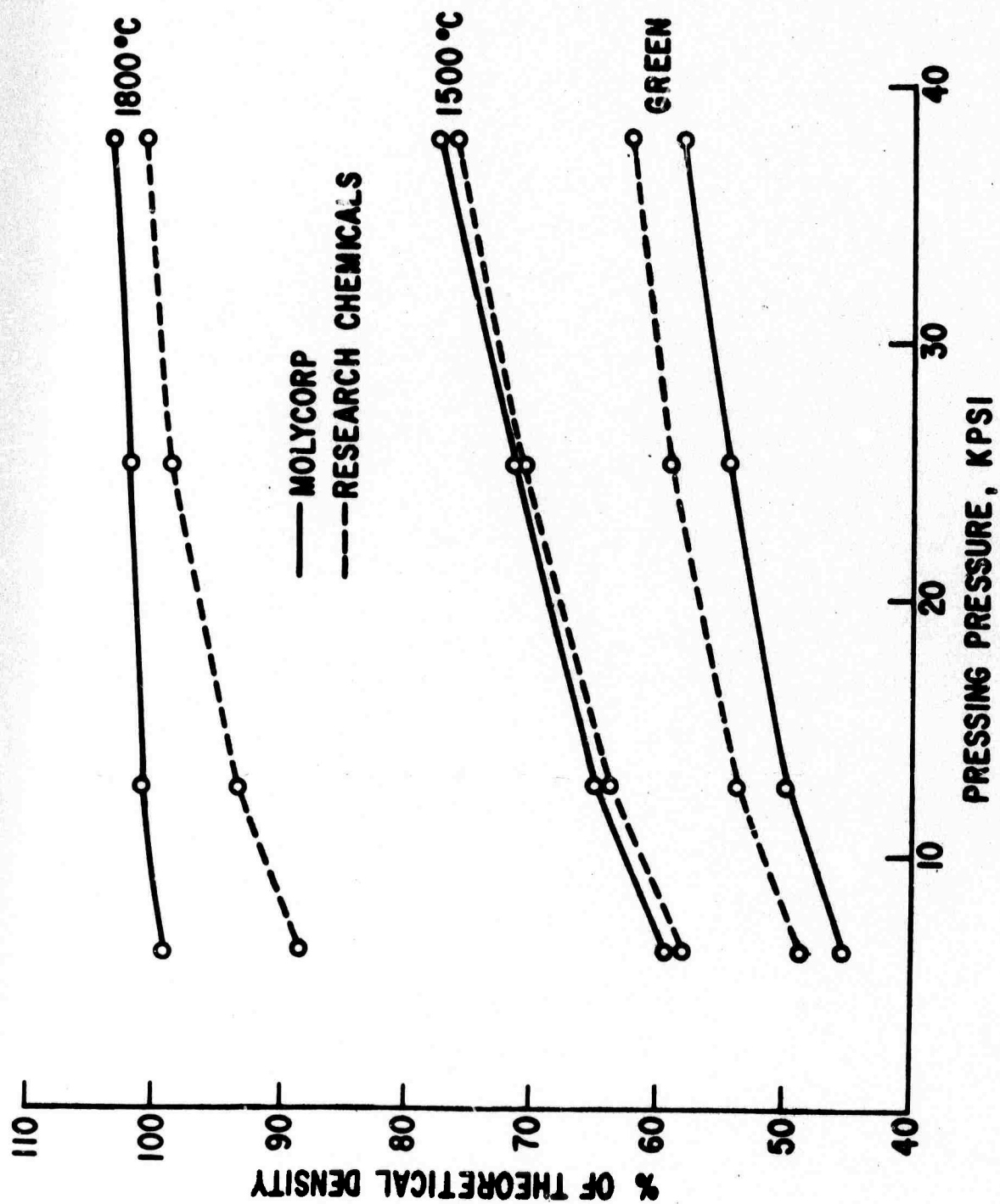
Figure 6. Percent Theoretical Density versus Pressing Pressure for Two Commercial
Y_2O_3 Powders Sintered for 16 hrs at 1500°C plus 21 hrs at 1800°C in H_2

As sintering occurs, however, the Molycorp powder sinters towards 100% theoretical density more rapidly than the Research Chemicals powder. This behavior is consistent with the smaller average particle size of the Molycorp powder.

The fact that the higher densities actually exceed 100% of the theoretical density is attributed to errors in the shrinkage measurements; the qualitative trend appears to be real.

An interesting extension of this series of experiments would be to measure the particle size distribution of the Alfa Y_2O_3 powder. According to the results of Fig. 3 and Fig. 4, it can be predicted that the Alfa powder will have an even smaller average particle size and distribution breadth than the Molycorp powder.

Although there are differences in the particle size distribution of the various Y_2O_3 powders, no correlation could be found between particle size and residual porosity in fired Yttralox samples.

3. Choice of Milling Technique

Three methods have been utilized to intimately mix the Y_2O_3 particles in the aqueous sulfate solution. They are (1) magnetic stirring with a Teflon coated stirring bar, (2) colloid milling in a stainless steel colloid mill, and (3) ball milling in a rubber lined ball mill containing Yttralox balls used extensively for the oxalate process.

Two Nd-doped Yttralox rods are shown in Fig. 7. They are illuminated by oblique light to reveal the internal optical defects. Both of these samples were processed in exactly the same way except that the sample on the right was made from colloid milled powder; the sample at the left was made from magnetically stirred powder. The magnetically stirred sample exhibits more porosity than the colloid milled sample, but the latter has a very visible haziness inside it.

The haziness associated with colloid milling is probably due to a metallic contamination from the colloid mill surfaces. Any reduction in residual porosity caused by the introduction of this haziness so that the overall transparency is equally poor in each sample. If a contaminant free colloid mill were available, a reduction in residual porosity might be realized.

One attempt was made to ball mill the sulfate powders in the rubber lined Yttralox ball mill. Samples made by this technique exhibited far more porosity than either the magnetically stirred or colloid milled samples. This finding was unexpected in view of the fact that ball milling reduces porosity in samples prepared by the oxalate process and is still not understood.

-15-
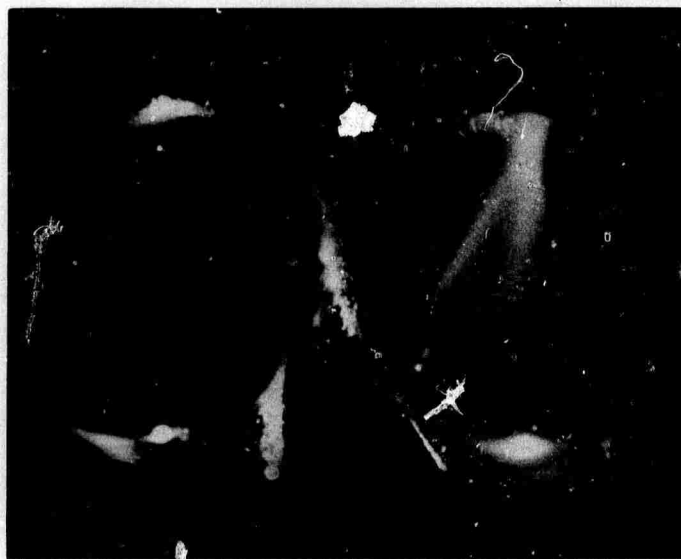
a)   b)

Figure 7. Effect of Colloid Milling on Transparency of Two
1/4" Diameter Yttralox Samples a) No Colloid
Milling, b) Heavily Colloid Milled

4. First Calcination Step

After the Y_2O_3 powder is thoroughly mixed into the aqueous sulfate solution, the entire solution is heated to dryness. The powder is then screened and calcined to convert the sulfates to oxides. Thermogravimetric analysis (TGA) of this calcination step is shown in Fig. 8. The weight loss below 400°C is due to the loss of water of hydration. For temperatures above 400°C three important observations can be made: (1) the Yttralox composition decomposes at a higher temperature than the pure $Th(SO_4)_2$ compound for the same atmosphere, (2) decomposition occurs at a lower temperature in H_2 than in air, and (3) pure $Th(SO_4)_2$ loses slightly less total weight in H_2 than in air.

It had been suggested in the second quarterly report that the higher temperature decomposition in the Yttralox composition was due to the formation of a thorium-yttrium sulfate during the aqueous chemistry part of the processing. To check this hypothesis a physical mixture of Y_2O_3 and $Th(SO_4)_2$ was analyzed and shown to exhibit the same high temperature decomposition as the standard Yttralox powders. It therefore appears that the decomposition of $Th(SO_4)_2$ to ThO_2 and SO_2 vapor in the presence of Y_2O_3 is stabilized to higher temperatures because of a solid-vapor reaction between the Y_2O_3 particles and the SO_2 vapor.

The TGA results showing that $Th(SO_4)_2$ decomposes at a lower temperature in H_2 than in air initially suggested the possibility of calcining Yttralox powders in H_2 at lower temperatures than is necessary in air. It was found, however, that large rods of Yttralox processed by calcination in H_2 frequently warped and even melted during firing treatments at temperatures below 2200°C. The tendency to warp and melt strongly suggested the presence of a liquid phase at the Yttralox grain boundaries.

As can be seen in Fig. 6, the total weight loss accompanying $Th(SO_4)_2$ decomposition is less in a H_2 atmosphere than in air. This indicates that a small amount of sulfide phase remains after a first calcination in H_2 and converts to a liquid phase during the high temperature firing treatment. An extensive amount of this second phase is shown in Fig. 9 in a sample which was calcined in H_2 before the high temperature firing treatment. In thin disk-shaped specimens, given a second calcination in air at 1350°C, this second phase material is not evident after firing. In thick cylindrically shaped rods, however, the sulfide phase cannot be removed as quickly during the second calcination in air and appears to be causing the sample to warp or melt during firing.

Evidence that the second phase material is sulfur rich is shown in Fig. 10, which is an electron microprobe, sulfur K_α display on an Yttralox sample heavily contaminated with the second phase material. Heavily concentrated regions of high sulfur content are apparent on the grain boundaries.
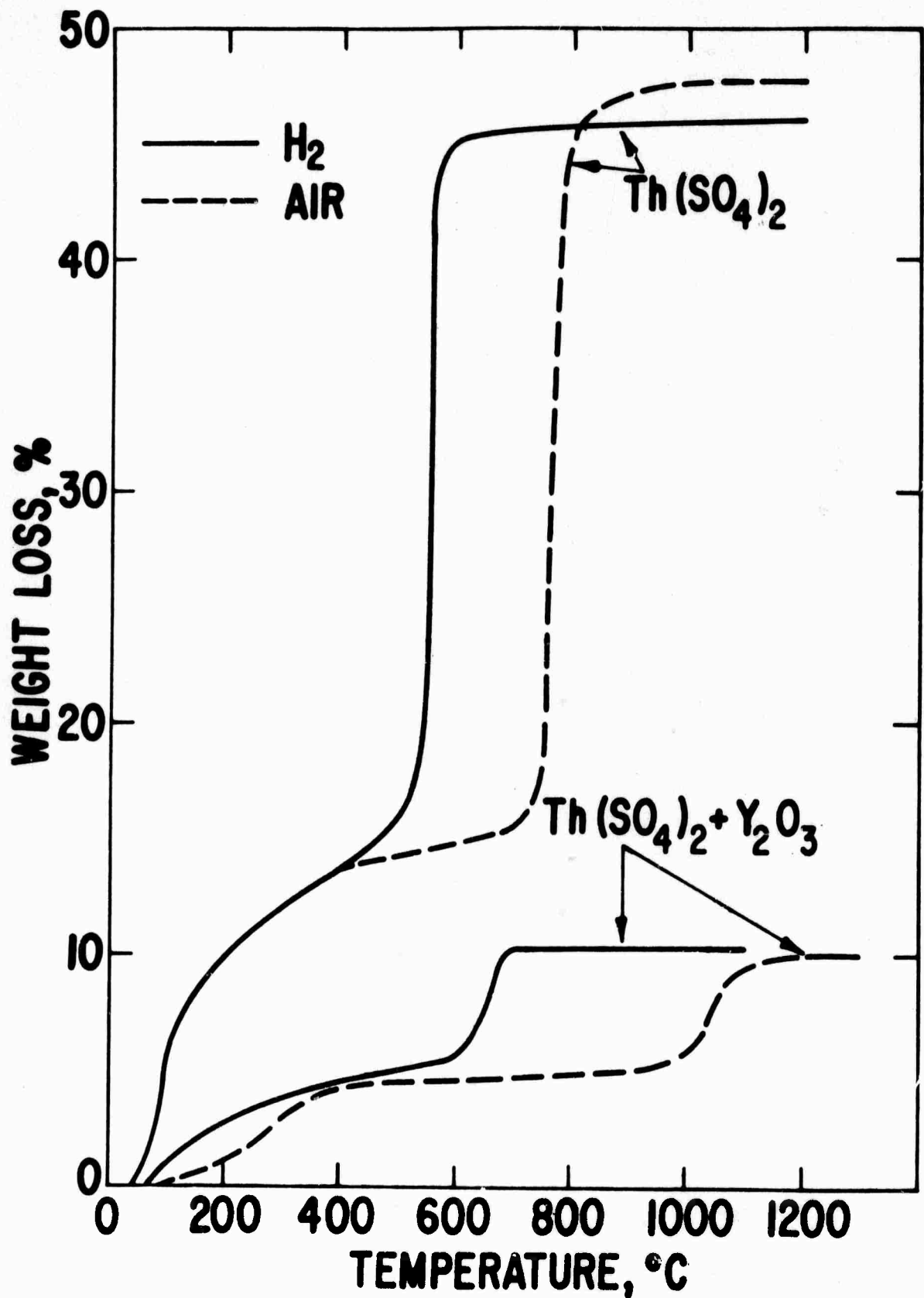
Figure 8. Thermogravimetric Analysis of $Th(SO_4)_2$ and Yttralox $(Th(SO_4)_2 + Y_2O_3)$ Powders Heated in H_2 and Air
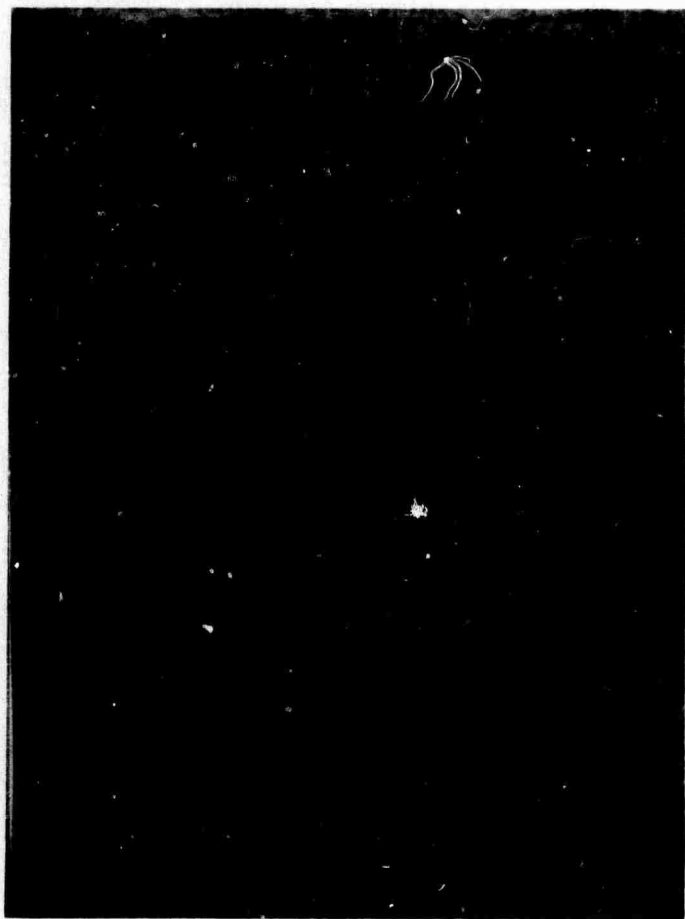
Figure 9. Grain Boundary Decoration in Yttralox Samples
Calcined in H_2 X137

NOT REPRODUCIBLE
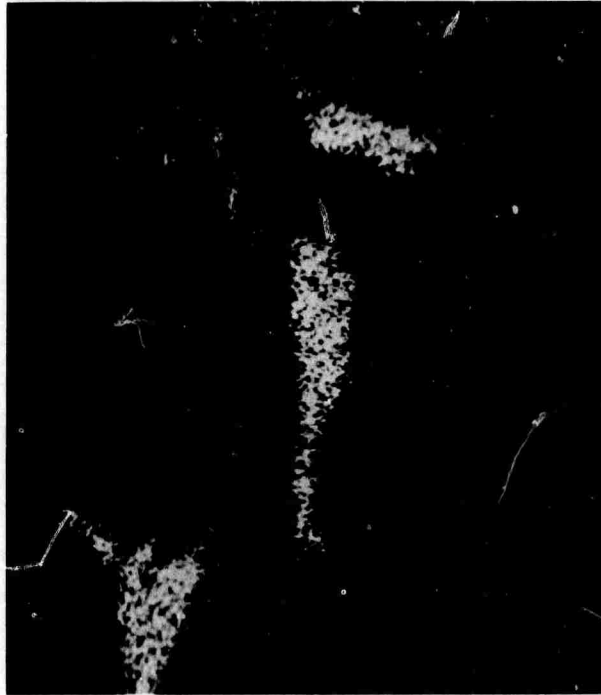
Figure 10. Electron Microprobe Scan of Sulfur K_α Peak from an Yttralox Sample Containing Excessive Grain Boundary Decoration   X1240

NOT REPRODUCIBLE

Since the second phase material is more stable in H_2 than in air, a TGA experiment was performed in which $Th(SO_4)_2$ was heated to 1000°C in H_2 and then cooled to room temperature in H_2. The gas atmosphere was then switched to N_2 and the sample reheated. During the heating in H_2, the sample lost 45.8% of its weight, and upon reheating in N_2, another 1-2% weight loss was observed between 100 and 400°C. This latter weight loss may be a sulfur-rich phase which is stable at 1000°C in H_2 but decomposes at much lower temperatures in a more oxidizing atmosphere. Its exact nature is not understood but this unknown phase is probably the cause of sample slumping and warping.

It is concluded that H_2 calcination of sulfate powders can be detrimental to Yttralox processing and should be avoided. Air or oxygen calcinations are preferable.

5. Second Calcination Step

The original laser rod made by the sulfate process utilized a 100 hour vacuum treatment at 1050°C after the rod was pressed into shape and before it was fired at high temperature. The results found during the present contract indicate that a 15 hour treatment in air at 1350°C yields an equally good specimen.

In one experiment the second calcination step consisted of a 15 hour treatment in vacuum at 1500°C. When this sample was fired, it had an opaque black surface layer over a transparent core. A tapered metallographic section through this black surface layer is shown in Fig. 11. The black surface layer is seen to consist of individual second phase particles. The origin or composition of these tiny particles is unknown. Until the effect of a vacuum calcination step is better understood, the second calcination step should not be done in vacuum.

6. Firing Procedure

All of the sintering treatments performed on sulfate powders during the present contract were done in a dry H_2 atmosphere at temperatures between 2080°C and 2175°C. Considerable amounts of porosity which existed after firing for 15 hours at 2100°C were readily eliminated when the same sample was subsequently fired at 2170°C for the same period of time. Longer firing times at the higher temperature eliminated even more of the pores less than about 10μ in diameter, but did not noticeably reduce the number of pores greater than 20μ in diameter.

One potentially disturbing observation occurred when a sintered rod was reheated for 15 hours at 1350°C in air. This sample, which exhibited no grain boundary decoration after the 2170°C firing in H_2, now revealed the very pronounced grain boundary decoration shown in Fig. 12. A subsequent firing in H_2 at 2100°C caused the grain boundary phase to disappear. The nature of this grain boundary phase may be caused by excess ThO_2 precipitating from solid solution or a sulfur-rich phase, as discussed previously.
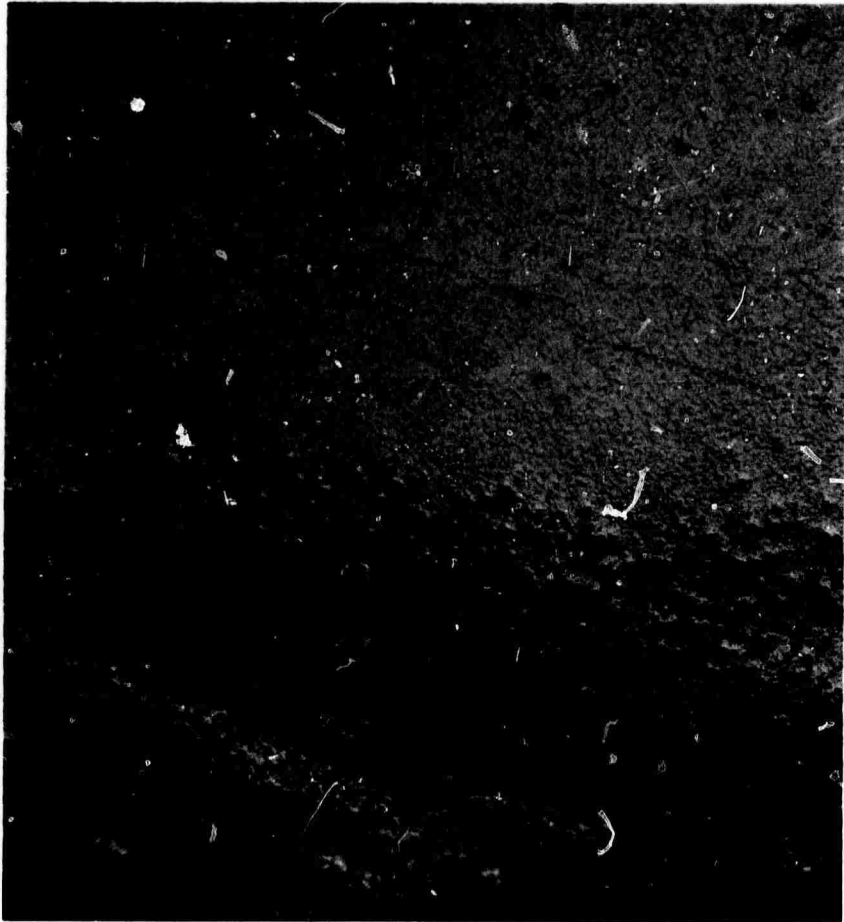
Figure 11. Tapered Section (10:1) Through Black Surface Layer
of Yttralox Sample Calcined in Vacuum at 1500°C X150

NOT REPRODUCIBLE

Figure 12. Grain Boundary Decoration in Sintered Sample Annealed
for 15 hrs at 1350°C in Air   X137

NOT REPRODUCIBLE

If prolonged lasing action should cause the grain boundary phase to appear, a potential problem may exist. The first laser rod made by the sulfate process two years ago eventually failed to lase because of a cloudiness or "solarization" induced by repeated lasing action. It is quite conceivable that solarization and the grain boundary phase are interrelated.

7. Conclusions

The sulfate process for making Yttralox laser rods will not be actively developed in the second contract. A description of the best sulfate processing technique achieved during the first contract is itemized in Appendix A. Further improvement in optical quality appears to be primarily limited by the purity of the starting Y_2O_3 powder. The residual porosity associated with impure Y_2O_3 powder is in the 20-50μ range and is strikingly insensitive to any of the processing steps. If further development were to be done on the sulfate process, it is suggested that the Y_2O_3 powder be synthesized from a water soluble yttrium compound such as yttrium sulfate.

B. Oxalate Process

1. Powder Synthesis

The oxalate synthesis method was developed with the aim of accomplishing the following conditions:

(1) Elimination of foreign impurity particles by the filtration of the starting liquids and by observing high standards of cleanliness during the ensuing processing steps.

(2) Homogeneous distribution of Th^{4+}, Y^{3+} and Nd^{3+} cations on an atomic scale thereby ensuring the chemical uniformity of the sintered material.

(3) Small particle size of powder processed into final specimens.

(4) Reduction of long heat treatment times required for sulfur elimination from powders prepared with sulfates.

Appropriate amounts of yttrium, thorium and neodymium nitrate were dissolved in filtered deionized water so that the final composition would be 89 mole % Y_2O_3, 10% ThO_2 and 1% Nd_2O_3. This salt solution was then filtered through Whatman #50 filter paper. Reagent grade oxalic acid, $H_2(C_2O_4) \cdot 2H_2O$ was added to filtered deionized water in a separate container such that the resulting solution was 80% saturated and contained a 100% excess of oxalic acid required to convert the Y-Th-Nd nitrates into oxalates. The acid solution was

also filtered in order to remove any foreign particulate matter. The salt solution was dripped into the oxalic bath while stirring with a Teflon coated magnetic stirring bar. This dripping procedure required about 2 1/2 hours. The resulting co-precipitated oxalate was washed with 54 liters of deionized water to increase the pH of the suspension to about 5-6. Subsequently, the oxalate precipitate was vacuum filtered and oven dried at 1100°C. Great care was taken to insure the highest degree of cleanliness during powder synthesis.

Particle morphology and size range were studied by scanning electron microscopy (SEM). The oxalate particles were approximately parallelopipeds with a size range between 0.3 and 3μ (see Fig. 13). X-ray diffraction techniques revealed that the precipitate was crystalline with an unidentified symmetry and structure.

2. Oxalate Decomposition and Calcination

A thermogravimetric analysis (TGA) study of the Y-Th-Nd oxalate powder in an air atmosphere is given in Fig. 14. Specimen weight loss below 300°C is probably caused by the loss of water from the oxalate powder (i.e. the chemical composition of the "oxalate powder" is probably a (Y-Th-Nd) oxalate-hydrate). The large weight loss between 300 and 600°C is attributed to the evolution of carbon mon- and di-oxides.

Presently, the first calcination step for the mixed oxalate powder is at 800°C for four hours in air. The SEM photomicrograph in Fig 15 reveals that there is a collapse of the well defined oxalate particles because of the 52% weight loss. The particle size range is similar to that of the uncalcined oxalate. In addition, a certain degree of agglomerate formation is evident and is probably caused by neck-growth between contacting particles by a sintering mechanism such as surface diffusion. Wilson and Shewmon[6] stressed that surface diffusion should dominate the neck-growth stage of sintering in several metals and Al_2O_3 at low temperatures and small particle sizes.

X-ray (Debye-Scherrer) photographs showed that the calcined powder consisted predominately of a Y_2O_3-ThO_2 crystalline solution plus a trace of free ThO_2. Either the interdiffusion kinetics are too slow for complete dissolution of ThO_2 into the Y_2O_3 structure at 800°C for four hours or thermodynamic equilibrium is established with the starting composition (Y_2O_3 + 10 mole % ThO_2) in a two phase region of the stability diagram (which is unknown.)

3. Sintering Unmilled Yttralox Powder

The adopted procedure for sintering Nd^{3+}-doped Yttralox disks or rods in a Brew furnace involves a heating cycle of 6-14 hours to 2170°C in dry H_2, a soak time from 10-125 hours at 2170°C in dry H_2 and a cooling cycle of 6 hours in wet H_2. After sintering, the specimens are ground and polished for observation and evaluation of the optical defects located within them.

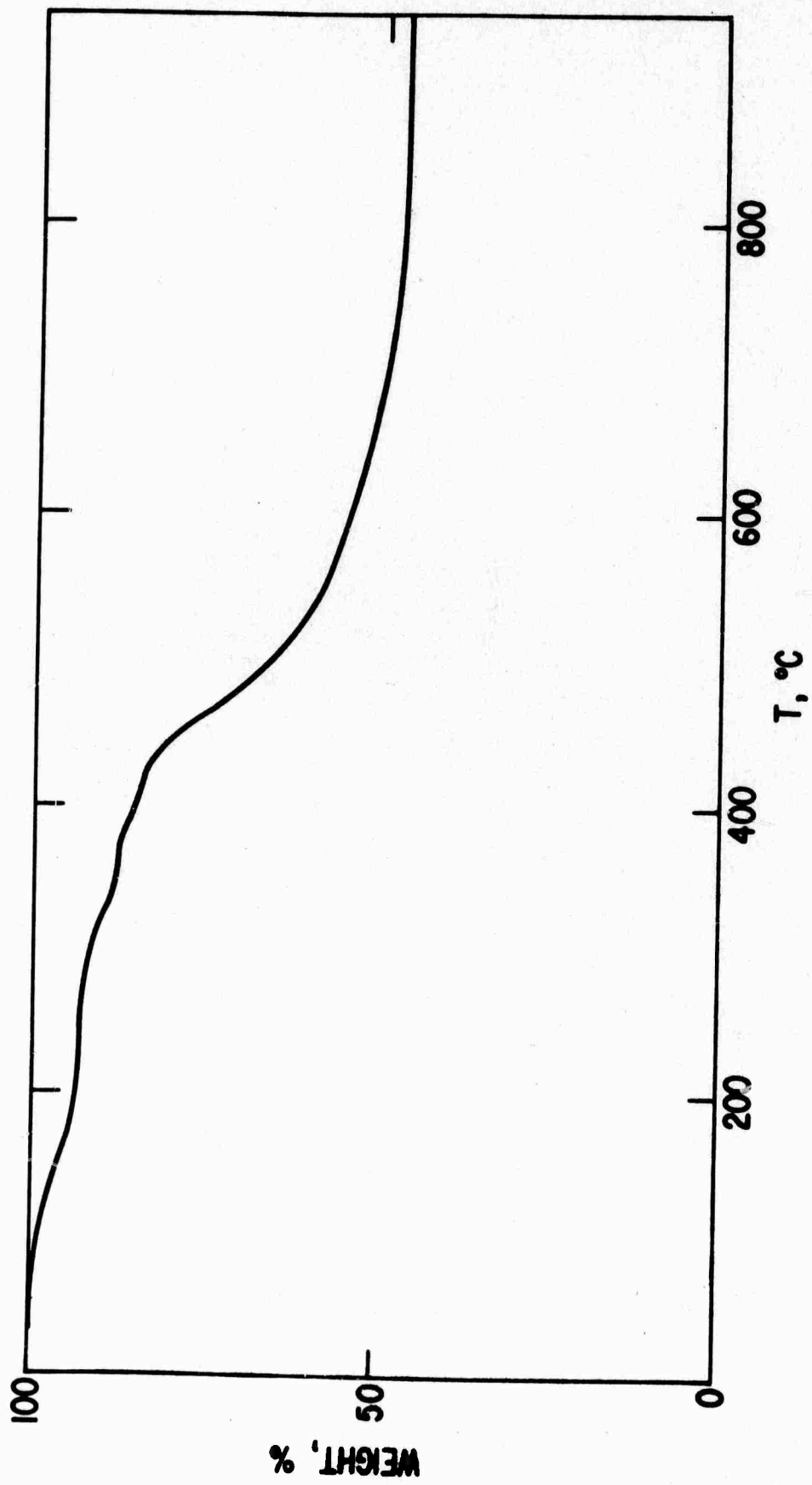Figure 14. TGA Curve for Yttralox Oxalate Powder

Figure 15. SEM Photomicrograph of Yttralox Oxalate Powder
            Calcined for 4 hrs at 800°C in Air   X5000

NOT REPRODUCIBLE

It has been established that if an oxalate powder is screened through a 100 mesh nylon screen, calcined at 800°C for four hours, isostatically compacted at 38 Kpsi and fired to 2170°C for 13 hours in the Brew furnace, there is less "orange peel" in the sintered specimen than if the powder were not screened. Since "orange peel" is a point to point variation in refractive index throughout the sintered specimen and probably arises from compositional gradients, a tentative explanation is that screening the oxalate powder before calcination breaks down agglomerates and makes the powder more (compositionally) uniform. All Yttralox prepared from the as-calcined oxalate powder has some "orange peel".

Porosity is another optical defect in addition to "orange peel". The quantitative determination of the porosity in a given Yttralox rod polished on both ends was easily accomplished with a petrographic microscope using a ruled graticule and white light. The technique involves (1) selecting three different magnifications at 30X, 80X and 285X, (2) scanning through known cylindrical volumes, (3) counting the number of pores and measuring their average size and (4) recording only pores with an average pore size greater than 22μ at 30X, between 4.5 and 22μ at 80X and between 0.5 and 4.5μ at 285X. Pores less than 0.5μ could not be detected. In general the total number of pores counted was approximately 100 to 200. The solid volumes analyzed at 30X, 80X and 285X were approximately 900 mm, 30 mm^3 and 3 mm^3 respectively. The average dimension of an occasional irregularly-shaped pore was determined by averaging the maximum and minimum linear dimensions (excluding tubular pores of which only 2 or 3 were observed in six rods). Pore volumes in various size ranges are then calculated, normalized to a standard total scanned volume of solid (i.e. μ^3 per mm^3) and plotted cumulatively on semi-log paper. Specimen preparation, counting, and calculating generally requires 1-2 days per specimen.

Cumulative porosity versus average pore size for a sintered Yttralox rod (YTC13-7) prepared from unmilled calcined powder is given in Fig. 16. A total porosity of 3.5×10^{-5} or 0.0035% is represented by the end point of the curve. The sharp rise of the curve between 1/2 and 5μ indicates an overwhelming majority of pores in this range. However, as the data points along the YTC13-7 curve indicate, there are some very large pores between 100 and 170μ. Although the cumulative porosity curve indicates very little about the spatial distribution of pores, some pore groups exist and consist of 3 to 20 tiny pores ($\approx 1-2\mu$) that are randomly located throughout the specimen. Because of the presence of 0.0035% porosity and a considerable degree of optical waviness or "orange peel", one cannot observe an object at the opposite end of a polished (YTC13-7) rod which is 2 1/2" long.
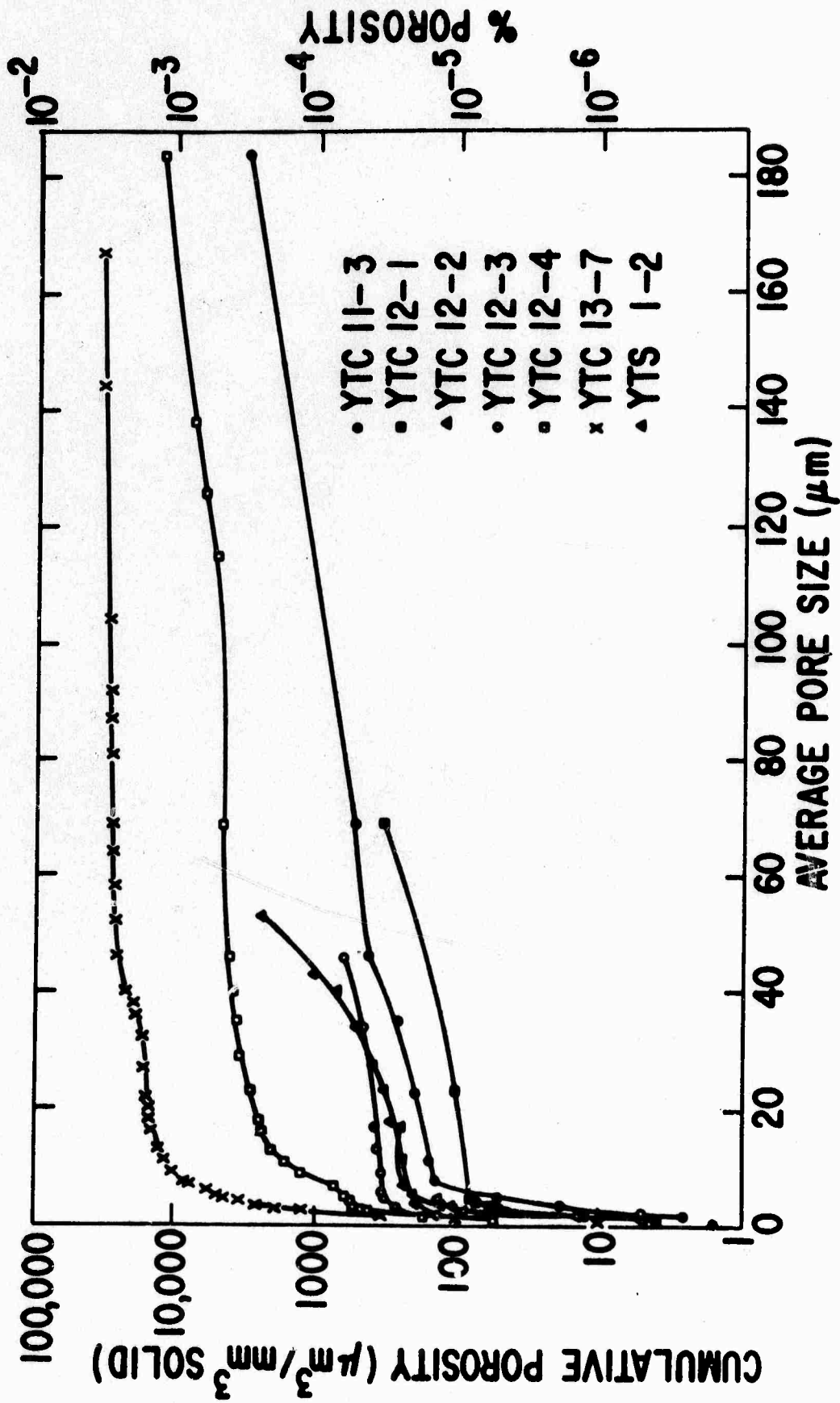
Figure 16. Cumulative Porosity Versus Average Pore Size for Selected Yttralox Rods

4. Sintering Ball-Milled Yttralox Powder

A "dry" ball milling operation was found to produce sintered Yttralox with high optical quality. Approximately 30 to 50 grams of calcined oxalate powder and 1 wt. % dry stearic acid are inserted into a rubber-lined ball mill containing Yttralox balls. After milling the calcined powder for six hours, the milled powder is carefully removed from the ball mill. The milled powder had a light yellowish tint to it and smelled like "rubber". Apparently the powder is picking up a small amount of rubber from the rubber lining of the ball mill. A SEM photomicrograph of the milled powder is illustrated in Fig. 17. The ultimate particle size is much less than 1μ and is of the order of 0.1μ. Although powder agglomerates prevail, these agglomerates are quite fragile and can be broken up when lightly squeezed between microscope slides.

The compactability of the milled powder was better than the unmilled powder. For example, the bulk green density of a powder compact prepared from milled powder was 60% theoretical whereas the bulk green density of a powder compact prepared from unmilled powder was only 52% theoretical at a forming pressure of 38 Kpsi. The higher the green density the smaller is the firing shrinkage and the less is the chance for cracking and distortion of the fired specimen. The better compaction of the milled powder particles is a good indication of a reduction in the number of agglomerates and large pores in the green compact. Large pores may give rise to residual porosity in the sintered piece.

A second calcination step above 1000°C in air is given to rod or disk-shape specimens previously pressed isostatically at 38 Kpsi from the milled powder. This processing step is used to burn-out stearic acid and rubber from the ball mill lining, and to decompose any free oxalate particles. Specimens are subsequently fired in the Brew furnace at 2170°C for 10 to 125 hours in dry H_2. The heat treatments used for 5 Yttralox rods prepared from milled powder are listed in Table II.

Sintered Yttralox rods were examined for their optical quality after polishing the rod ends with diamond paste. A striking discovery was that one could clearly see through a 3" long rod and focus on an object at a distance of 1 or 2 miles. All rods were very transparent and contained a few optical defects which were visible with the unaided eye. Furthermore, there was very little "orange peel" in the sintered rods. The large reduction of "orange peel" in sintered Yttralox prepared from ball milled powder is illustrated in Fig. 18. In a given sample "orange peel" can be observed at low magnifications with the optical microscope by using a pinhole source of transmitted white light. It is qualitatively evidenced by a black and white "grainy" appearance when the specimen surface is viewed slightly out of focus.
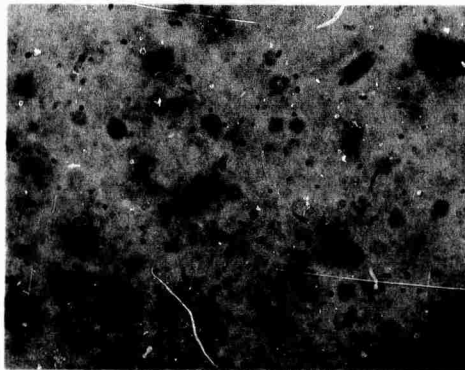
Figure 17. SEM Photomicrograph of Ball-Milled Yttralox
Powder   X10,000

(a)

(b)
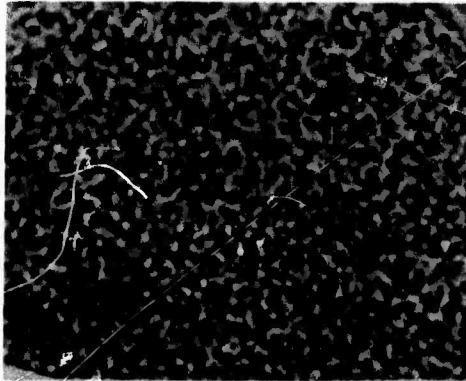
Figure 18. Orange Peel in Yttralox Prepared from (a) Unmilled
and (b) Milled Powder

TABLE II

FIRING SCHEDULE FOR YTTRALOX RODS PREPARED FROM MILLED POWDER

Sample	2nd Calcination Step	Heat-up Time to 2170°C	Soak Time at 2170°C
YTC11-3	1100°C-2 hours, air	6 hours	58
YTC12-1	1100°C-2 hours, air	6 hours	125
YTC12-2	1100°C-2 hours, air	6 hours	125
YTC12-3	1100°C-2 hours, air	13.5 hours	108
YTC12-4	1350°C-2 hours, air	13.5 hours	108

A plot of cumulative porosity versus average pore size for each sintered rod prepared from ball milled powder is given in Fig. 16. These sintered rods have less total porosity than rod YTC13-7 which was prepared from unmilled powder. The total porosity ranges from about $1.2 \times 10^{-3}\%$ for rod YTC12-4 to about $2.5 \times 10^{-5}\%$ for rod YTC12-3. A comparison of the total porosity in rods YTC13-7 and YTC12-3 shows that porosity can be reduced by approximately two orders of magnitude if the Yttralox powder is ball-milled and the appropriate heat treatment designated in Table II is followed. It is evident that there is a variation in residual porosity and pore size distribution with changes in the heat treatment of a rod.

The majority of pores for all sintered rods represented in Fig. (16) falls in the size range between 0.5μ and 5μ. Plots of pore frequency versus average pore size for rods YTC12-1 and YTC12-4 are given in Figs. (19) and (20), respectively. The size of nearly all pores falls between 0.5μ and 5μ in rod YTC12-1. On the other hand, the majority of pores in rod YTC12-4 also falls within the 0.5 to 5μ range but there is a considerable number of pores which have average pore sizes as large as 40μ. A few pores larger than 40μ, although small in number, increase the pore volume in rod YTC12-4 by a substantial amount (see Fig. 16). Pores larger than 40μ in size were omitted from Fig. 20 for the sake of convenience.

Another optical defect that can be identified in sintered Yttralox prepared from calcined oxalate powder which was milled is a small amount of second phase that wets the grain boundaries. This grain boundary decoration phase, which is found only in specimens prepared from milled oxalate powder, is similar to that observed in sintered Yttralox prepared by the sulfate technique. Electron microprobe data has unequivocally identified grain boundary decoration in Yttralox prepared by the sulfate process as a second phase containing a considerable amount of sulfur (see Fig. 9).
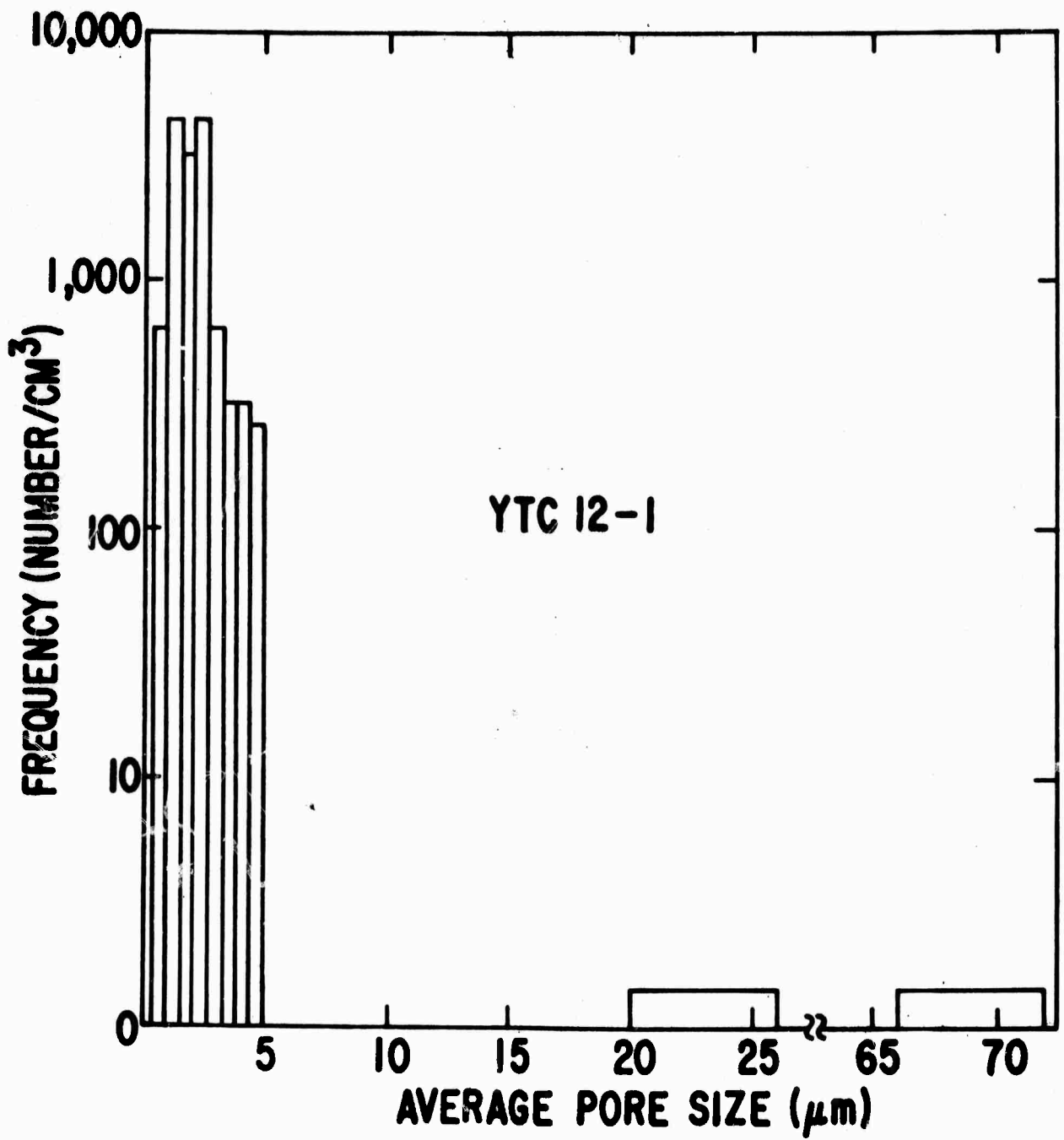
Figure 19. Pore Frequency Versus Average Pore Size for YTC12-1 Rod
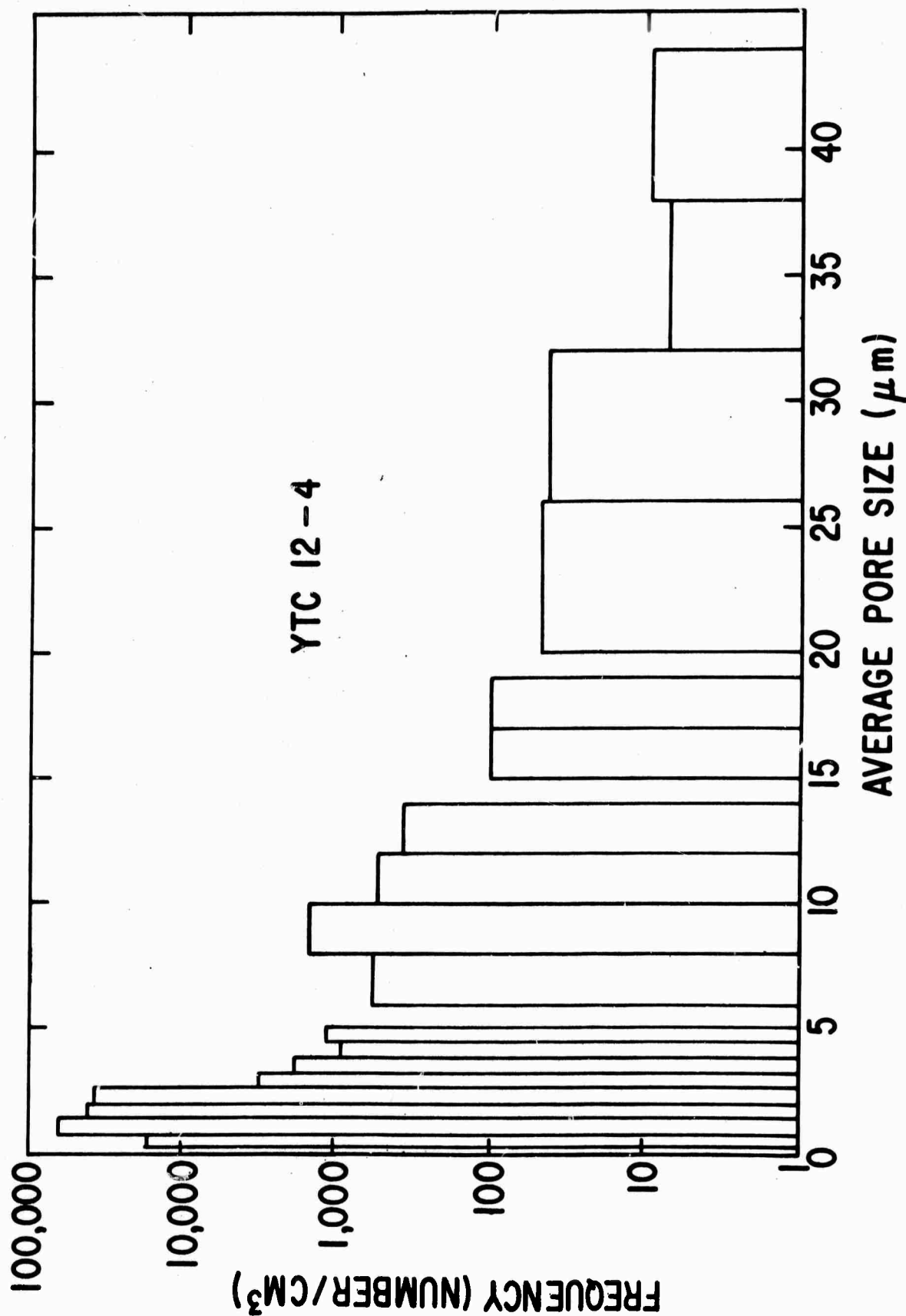
Figure 20. Pore Frequency Versus Average Pore Size for YTC12-4 Rod

The sulfur content in samples after various stages of powder processing and sintering treatment is determined by a standard high temperature combustion test. The results are given in Table III and show that the source of sulfur is the Yttralox ball mill. Approximately 0.22 wt. % sulfur is taken into the Yttralox powder after ball milling for 6 hours. The sulfur contamination originates either from the rubber lining of the ball mill or from the Yttralox balls which were prepared by the sulfate process. In any case, the sulfur concentration can be virtually eliminated by extended firing times at high temperature (sample 4). An extended investigation on the exact source of sulfur and on the absolute value of the sulfur concentration versus milling time is currently underway.

TABLE III

SULFUR CONTENT IN YTTRALOX AFTER VARIOUS STAGES
OF POWDER PROCESSING OR SINTERING TREATMENT

Sample	Powder Processing	Sintering Treatment	Sulfur Content (ppm)
1	oxalate powder, calcined 4 hrs-800°C	----	40
2	ball-milled calcined powder, 6 hrs.	----	2200
3	ball-milled calcined powder, 6 hrs.	11 hrs - 2115°C	370
4	ball-milled calcined powder, 6 hrs.	125 hrs - 2170°C	40

C. Yttralox Laser Results

1. Experimental Set-up

A preliminary evaluation of the laser characteristics of 5 rods was carried out. The rods measured 4 mm in diameter by 3 inches in length. The laser pump cavity was of the exfocal type with a second surface silver reflector measuring 3/4 inch in diameter by 2 1/2 inches in length. The pump lamp was an EG&G 4 mm bore 3 inch-long Xenon lamp, producing a pump pulse of approximately 100 sec duration. The laser resonant cavity consisted of a 100% dielectric mirror with a radius of curvature of 4.66 meters and a flat output mirror spaced 30 cm apart.

It was discovered before the contract began that the unfiltered pump light would solarize the Yttralox rods and that this could be prevented by surrounding the Yttralox rod with a Schott yellow glass filter cutting off at approximately 5000Å wavelength. All measurements reported here were performed with this filter in place.

-37-

2. Laser Threshold

Laser threshold measurements on Nd-doped Yttralox rods were carried out using a 95% reflectivity output mirror. For comparison threshold measurements were also made on a Nd-doped YAG rod and a rod of OI ND-11 laser glass. The pump energy required to achieve laser threshold was as follows:

YAG = 1.25 Joules
ND-11 Glass = 15 Joules
Yttralox YTC12-1 = 28 Joules
Yttralox YTC12-2 = 32 Joules
Yttralox YTC11-3 = 60 Joules
Yttralox YTC12-4 = 50 Joules
Yttralox YTS1-2 = 50 Joules

Yttralox rod YTS1-2 was not produced during the current contact but was the first laser rod made approximately two years ago by the sulfate process. It originally had a threshold about half this value but was solarized by being pumped without a filter. Upon being reannealed the rod cleared up but did not return to its original color.

A comparison of the laser threshold values with the total porosity content for various Nd-doped Yttralox rods is given in Table IV. A laser threshold value could not be obtained for specimen YTC12-3 because this Yttralox rod was broken during the machining of the rod.

TABLE IV

RESIDUAL POROSITY AND LASER THRESHOLD FOR VARIOUS
Nd-DOPED YTTRALOX RODS

Sample	Residual Porosity (%)	Laser Threshold (joules)
YTC11-3	3.2×10^{-4}	60
YTC12-1	3.3×10^{-5}	28
YTC12-2	2.5×10^{-5}	32
YTC12-3	6.6×10^{-5}	--
YTC12-4	1.2×10^{-3}	50

3. Efficiency

The output energy of the lowest threshold rod, YTC12-1, was measured for 3 different output reflectivities. The results are shown in Fig. (21). With a 50% output mirror this rod exhibited a slope efficiency of 0.1%.
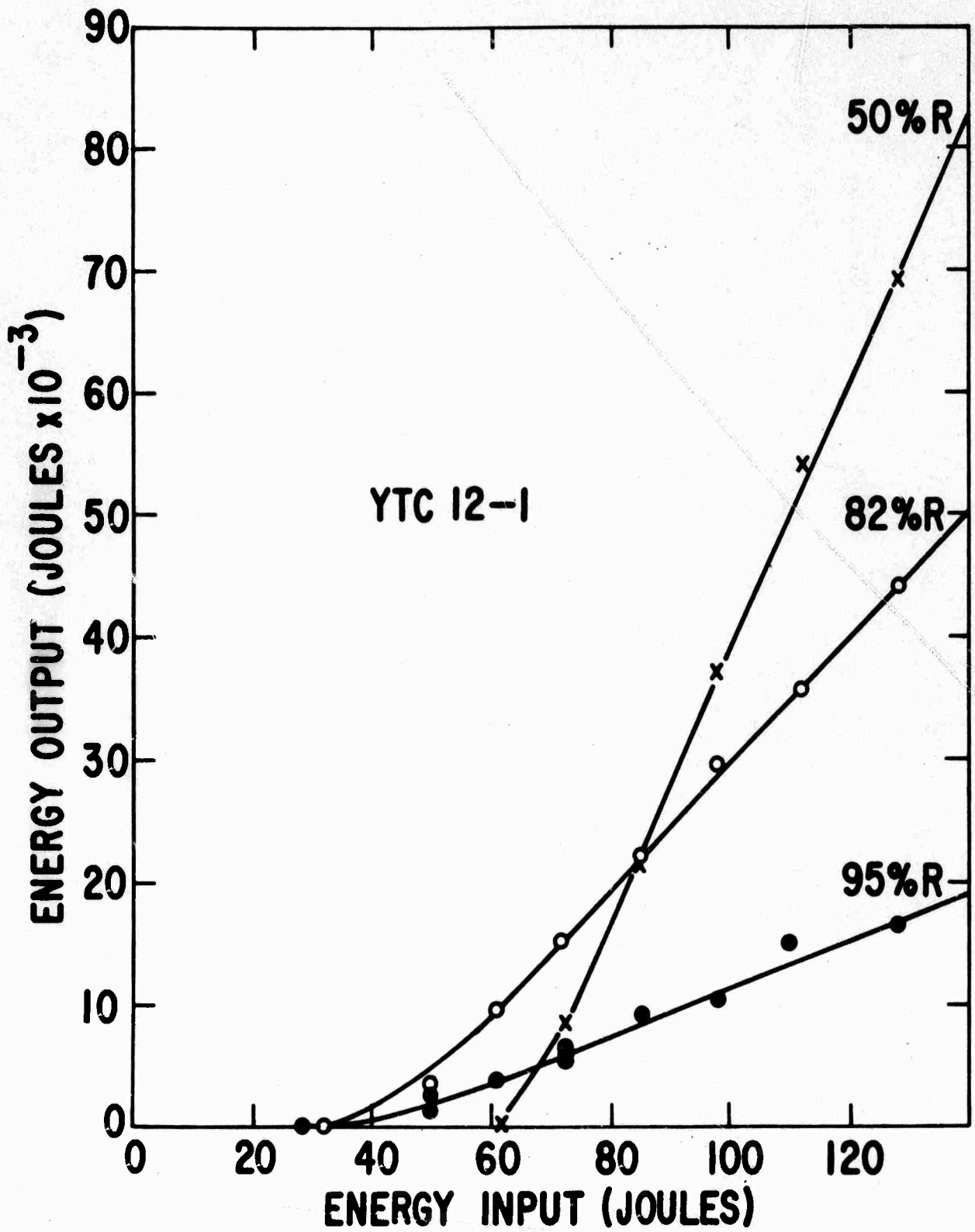
Figure 21. Energy Output Versus Energy Input for Different
Output Reflectivities for YTC12-1 Rod

4. Loss Coefficient

The loss coefficient (γ) can be determined from the threshold values for different mirror reflectivities. At threshold there is the requirement that $1/R = 3^{(\sigma n-\gamma)2L}$, σ being the stimulation cross section, n the inversion density and 2L the path length. If ln 1/R is plotted as a function of pump energy and extrapolated to zero pump power giving n=0, the intercept with the ordinate gives ln $1/R = -\gamma 2L$. From this technique it is inferred that the loss coefficient for Yttralox rod YTC12-1 is of the order of 2% per cm.

D. Discussion

During the present contract the major effort was directed at controlling and improving the ceramic processing needed to prepare Nd-doped Yttralox laser rods. The two basic processing methods which were developed simultaneously were the sulfate and oxalate processes. Although the sulfate process was unsuccessful in producing an Yttralox rod that lased, the oxalate process in combination with an Yttralox ball mill did produce laser-quality rods. The recommended procedure for making laser-quality rods by the oxalate process is given in appendix B.

It has been pointed out that if calcined Y-Th-Nd oxalate powder is ball milled before sintering there is a reduction in the amount of "orange peel" in the sintered ceramic. It is rationalized that by ball milling there is a breakdown of agglomerates, a particle size reduction and a chemically more homogeneous powder results. Such a powder gives rise to reduced concentration gradients on a local scale in the sintered piece and to a faster approach to thermodynamic equilibrium. This strongly suggests that "orange peel" is caused by concentration gradients. We plan to quantify this optical effect by measuring interferometric fringe displacement.

A major optical defect in sintered Yttralox is porosity. There are several very large pores greater than 50μ which are found in sintered Yttralox prepared from both unmilled and ball milled powders (see Fig. 16). Observation of the large pores with an optical microscope using transmitted light reveals that their frequency is higher in Yttralox prepared from unmilled powder. Occasionally a very large pore $\approx$ 100 to 200μ in size has a galaxy of smaller pores surrounding it. These large pores may originate from (1) incomplete decomposition of the starting oxalate powder which has been formed into a ceramic body. (In some cases the evolution of CO and CO_2 during the final stages of sintering can stabilize pores by gas entrapment in that region from which the gas originated), (2) large voids formed from bridging of agglomerates in the green piece, (3) pore growth caused by the migration of pores along with the grain boundaries and (4) decomposition of foreign matter such as lint particles, stearic acid and rubber. The fact that ball milled Yttralox powder has a smaller particle size, has a higher packing density and is more compositionally uniform than unmilled powder indicates that possibility (4) may be the main reason for the presence of very large pores in sintered Yttralox prepared from ball milled powder. Such large pores are very stable and firing the same specimen for times longer at 2170°C does not cause a noticeable decrease in their size. (10)

Figure 16 illustrates that all sintered rods prepared from ball milled powder have less residual porosity than in rod YTC13-7 which was prepared from unmilled powder. A reduction in porosity of about two orders of magnitude (compare YTC13-7 and YTC12-1) is thought not to be primarily due to a better dispersion of the ThO_2 sintering aid but to be caused by the sulfur contamination during the ball milling operation (see Table II). Since sulfur segregates at the grain boundaries, this strongly suggests that the grain boundary mobility when sulfur is present is less than or equal to the pore mobility and pores can preferentially disappear faster than if sulfur were absent.

The influence of the firing schedule of the Yttralox rods prepared from milled powder given in Table II on the resulting residual porosity of the same rods shown in Table IV can be explained if it is assumed that the segregation of sulfur on the grain boundaries retards grain growth and permits pore elimination. A comparison of rods YTC12-3 and YTC12-4 shows that the firing schedules were identical except that YTC12-3 had a second calcination step at 1100°C and YTC12-4 had a second calcination step at 1350°C. The higher temperature used for the second calcination step for YTC12-4 probably burned out a substantial amount of sulfur from the powder compact and resulted in a specimen containing about 20 times as much porosity. Similarly, a comparison of YTC12-2 and YTC'.-3 rods shows that by extending the heat-up time to 2170°C from 6 to 13.5 hours, the residual porosity increases from 2.5 x 10⁻⁵% to 6.6 x 10⁻⁵%. Again, the longer heat-up time probably removes more sulfur such that a certain amount of exaggerated grain growth can take place with pores trapped inside the grains. Rods YTC12-1 and YTC12-2 had identical firing schedules and nearly the same residual porosities. Although rod YTC11-3 had nearly the same firing schedule as YTC12-1 and YTC12-2 rods except for the shorter soak time at 2170°C, its porosity was nearly a factor of 10 higher. A close examination of rod YTC11-3 under the optical microscope shows that two large pores greater than 50μ in size found in a solid volume of 1.3 cm³ drastically increased the porosity from 4.2 x 10⁻⁵% to about 3.2 x 10⁻⁴%. Therefore, if these two large pores (probably formed by the decomposition of foreign particulate matter) were excluded in YTC11-3, the final porosity of YTC11-3 would be nearly that of YTC12-1 and YTC12-2.

The majority of pores found in all Yttralox rods are generally in the size range between 0.5μ and 5μ. (At the present time pores smaller than 0.5μ have not been counted.) The pore size distribution can be very narrow as in the case of YTC12-1 (Fig. 19) or very broad as in the case of YTC12-4 (Fig. 20). There are about 4,000 pores per cm³ at about 1.2, 1.8 and 2.4μ pore sizes in YTC12-1 whereas there are about 40,000 or more pores per cm³ for the same pore sizes in YTC12-4. After consideration of the total number of pores of all sizes per cm³, the average pore spacing was about 410μ in YTC12-1 and about 180μ in YTC12-4. If the vacancy diffusion path length is roughly equal to one half of the pore spacing during final stages of densification, then these

large diffusion path lengths will certainly give rise to very slow densification kinetics depending, of course, on whether or not a given pore is on the grain boundary. Pores greater than 40_μ are almost always on the grain boundary whereas pores less than 10_μ appear to be located inside grains. (The average grain size for most Yttralox rods was about 140_μ).

All Nd-doped Yttralox rods prepared from ball milled powder exhibit lasing action. The laser threshold values and the residual porosity of each rod is listed in Table IV. YTC12-1 and YTC12-2 have nearly the same porosity ($\approx 3 \times 10^{-5}$%) and about the same laser threshold value (≈ 30 joules). As the residual porosity increases to $\approx 10^{-3}$% (YTC12-4), the laser threshold value also increases to about 50 joules. Specimen YTC11-3 falls out of sequence with the "higher residual porosity--higher laser threshold" trend because it contains an additional optical defect which is grain boundary decoration. Although YTC11-3 has about 1/4 the residual porosity as YTC12-4, it has a higher threshold value (≈ 60 joules) because of the presence of this grain boundary decoration. It appears that the segregation of sulfur at the grain boundaries is helpful for pore elimination but the retention of the liquid phase at the grain boundaries is detrimental to the lasing behavior of the specimen. Fortunately grain boundary decoration appears to be removed by prolonged firing at temperatures between 2000°C and 2200°C.

The determination of a loss coefficient and an efficiency for Yttralox rod YTC12-1 shows that the loss coefficient is of the order of 2% per cm and an efficiency of about 0.1%. A neodymium-doped glass rod has a loss coefficient of about 0.2-0.4% per cm and an efficiency of about 1%. Therefore, Yttralox ceramic lasers are presently about an order of magnitude inferior to glass with respect to loss coefficient and lasing efficiency. Considering the improvement in optical perfection that the Yttralox ceramic laser program has demonstrated during the past year, the probability of reproducibly synthesizing Yttralox lasers is large. It is estimated that another order of magnitude reduction in porosity is required to produce Yttralox with a lasing efficiency comparable to that of Nd-doped optical glass.

V.   APPENDIX A

Recommended Sulfate Technique

1) Suspend 89 mole % Y_2O_3 powder (99.99% pure) in deionized water and vacuum screen it through -140 mesh nylon screen.

2) Dissolve the appropriate amounts of $Th(SO_4)_2$ and $Nd_2(SO_4)_3$ (10 mole % ThO_2 and 1 mole % Nd_2O_3, respectively) in deionized water and filter through a hard filter paper.

3) Mix the two solutions and stir vigorously in a magnetically stirred beaker.

4) Heat the stirring mixture on a hot plate and reduce to dryness as rapidly as possible without causing violent boiling.

5) Dry the powder for 6-12 hours in air at about 110°C.

6) Screen the dry powder through -100 mesh nylon screen.

7) Calcine the powder in an open Al_2O_3 boat for seven hours at 1000°C in flowing air.

8) Die press or isostatically press the powder into the desired configuration at approximately 40,000 psi.

9) Calcine the pressed sample for 15 hours at 1350°C in flowing air.

10) Fire the sample for at least 48 hours at 2170°C in dry H_2.

11) Cool the sample to room temperature in wet hydrogen (dew point ~25°C).

The above procedure should yield transparent specimens less than 1 cm thick, but will not yield the degree of transparency necessary to make a 3" long rod lase.

VI.   APPENDIX B

Recommended Oxalate Technique

1)   Dissolve appropriate amounts of yttrium, thorium and neodymium nitrate in filtered deionized water to make a final composition of 89 mole % Y_2O_3, 10% ThO_2 and 1% Nd_2O_3.

2)   Filter the solution through Whatman #50 filter paper.

3)   Dissolve an appropriate amount of oxalic acid in filtered deionized water so that the solution is 80% saturated and contains 100% excess oxalic acid required to convert the Y - Th - Nd nitrates into oxalates.

4)   Filter the oxalic acid solution.

5)   Drip the salt solution into a stirred solution of oxalic acid.

6)   Wash the co-precipitated oxalate with filtered deionized water.

7)   Vacuum filter the oxalate precipitate.

8)   Dry the powder for 6-12 hours in air at 110°C.

9)   Calcine the powder at 800°C for 4 hours in air.

10) Dry ball mill the calcined powder plus 1 wt. % stearic acid for 6 hours in a rubber lined ball mill containing Yttralox balls.

11) Isostatically press rod-shape specimens at about 40 Kpsi.

12) Calcine the rods at 1100°C for 2 hours in air.

13) Use a six hour heating cycle to 2170°C in dry H_2.

14) Fire rods at about 2170°C in dry H_2 for about 50-125 hours.

15) Cool specimens in 6 hours to room temperature in wet H_2 (dew point $\sim$ 25°C).

VI. REFERENCES

1. P. J. Jorgensen and R. C. Anderson, "Grain-Boundary Segregation and Final-Stage Sintering of Y_2O_3," J. Am. Ceram. Soc., 50 (11) 553-558 (1967).

2. J. E. Burke, "Role of Grain Boundaries in Sintering," J. Am. Ceram. Soc., 40 (3) 80-85 (1957).

3. R. L. Coble, "Initial Sintering of Alumina and Hematite," J. Am. Ceram. Soc., 41 (2) 55-62 (1958).

4. D. Lynn Johnson and Ivan B. Cutler, "Diffusion Sintering: I. Initial Stage Sintering Models and Their Application to Shrinkage of Powder Companys," J. Am. Ceram. Soc., 46 (11) 541-550 (1963).

5. R. L. Coble, "Sintering Crystalline Solids. I. Intermediate and Final State Diffusion Models," J. Appl. Physics, 32 (5) 787-792 (1961).

6. T. L. Wilson and P. G. Shewmon, "The Role of Interfacial Diffusion in the Sintering of Copper," Trans. Met. Soc. AIME, 236 48-58 (1966).

7. S. Prochazka and R. L. Coble, "Surface Diffusion in the Initial Sintering of Alumina - Part III - Kinetic Study", Physics of Sintering, 2 (2) 15-33 (1970).

8. M. Hillert, "On the Theory of Normal and Abnormal Grain Growth," Acta Met., 13 (3) 227-238 (1965).

9. D. Lynn Johnson and T. M. Clarke, "Grain Boundary and Volume Diffusion in the Sintering of Silver," Acta Met., 12 (10) 1173-79 (1964).

10. W. D. Kingery and B. Francois, "Grain Growth in Porous Compacts," J. Am. Ceram. Soc., 48 (10) 546-47 (1965).